NMBU

Numerical investigation of the flexural behavior of timber-concrete composite floor systems.

M30-BA Master Structural Engineering and Architecture- H23

Mohand Morchid Alhussain

Preface

This thesis was written in December 2023, as a graduation thesis of a master's study in Structural Engineering and Architecture at the Norwegian University of Life Sciences. The thesis investigates the numerical analysis of the flexural behavior of timber-concrete composite floor system linearly supported at two edges and subjected to a four-point bending test. The numerical analysis is validated by a physical experiment and conducted with the use of a FEM-software.

The motivations behind this thesis are the interest in timber constructions; that has had strong traditions in Norway throughout the years, and the interest in finite element analyses. In addition, there is growing attention in combining timber with concrete for greener and more sustainable structural engineering techniques. Timber is an organic sustainable construction material and reducing the volume of concrete in multistorey building will contribute into achieving the global sustainability goals.

The idea behind this thesis was introduced by Associate Professor Themistoklis Tsalkatidis, who has provided guidance and supervision throughout the whole semester.

The deepest appreciations and the most gratitude to Associate professor Themistoklis Tsalkatidis for his kind guidance during this work.

Finally, I want to thank my father, mother, wife and my children Sara, Ali and Sirin for the huge motivation they have always given me, to keep setting the bar high and looking for achieving great goals.

Mohand Morchid Alhussain

Mohand Morchid Alhussain

Ås, Norway

December 15th, 2023

Abstract

The interest in combining concrete with timber into "timber-concrete composite structures" has grown significantly in recent years. Connecting these two materials in composite structures has provided the advantages of both timber and concrete and contributed to a more sustainable structural engineering technique. Norway is one of the most sustainable countries in the world and has always placed a high emphasis on creating a greener society and preserving the natural environment. There are many advantages in using timber-concrete composite structures opposed to pure concrete, such as the reduction of the dead-load and CO_2 emissions. Timber is a natural organic sustainable material; therefore, it is sustainable to replace some of the concrete's volume with timber.

The aim of this thesis is to further advance the research on timber-concrete composite (TCC) structures, by conducting a finite element analysis (FEA) of a TCC floor system. The TCC floor system consists of a beam-frame of glued laminated timber overlayed by a 70 mm thick concrete slab. The numerical analysis is validated by the results of a physical experiment by Ferrara et al. (2023) of the flexural behavior of a TCC floor system subjected to a four-point bending test.

The FEM-software used in this numerical analysis was ANSYS Mechanical APDL R2 2023. The numerical analysis of the TCC floor system was challenging, due to the orthotropic nature of timber and the requirement of calculating the mechanical properties of the glulam beams. The FEA analysis with produced a quite accurate result. This further allowed for an advanced investigation, in the form of three parametric studies. The effect, of these different parameters of the TCC floor system, on the result were analyzed. The first parametric study investigated the influence of the thickness of concrete slab on the maximum displacement, von Mises stresses and the total stresses in the contact elements. Moreover, the second parametric study examined the effect of the strength class of glulam beams, while the third parametric study analyzed the influence of the load placement. The results of the parametric analyses showed that the thickness of the concrete slab is crucially effective on the maximum displacement and the stresses in TCC floor systems. Increasing the thickness of concrete slab by 20 mm resulted in reducing the maximum displacement by 10 % and the stresses by 14 %. On the other hand, moving the concentrated loads from the mid-span and placing the loads towards the supports decreased the maximum displacement by 29 % and the stresses by 33 %.

Further work involving the effect of the thickness of the concrete slab on the natural frequency and vibration of the floor system is recommended for deeper knowledge of the performance of timber-concrete composite floor systems.

Sammendrag

Interessen i å kombinere betong med tre til "tre-betong hybridkonstruksjoner" har vokst betydelig i de siste årene. Å koble disse to materialene sammen, i komposittstrukturer har gitt fordelene til både tre og betong og bidratt til en mer bærekraftig konstruksjonsteknikk. Norge er et av verdens mest bærekraftige land og har alltid lagt stor vekt på å skape et grønnere samfunn og bevare naturen. Det er mange fordeler ved å bruke tre-betong komposittkonstruksjoner i motsetning til ren betong, for eksempel reduksjon av egenlast og CO_2-utslipp. Tre er et naturlig organisk bærekraftig materiale; Derfor er det bærekraftig å erstatte noe av betongens volum med tre.

Målet med denne masteroppgaven er å fremme forskningen på tre-betong Hybridstrukturer, ved å gjennomføre en endelig elementanalyse (Finittelementmetoden) på et tre-betong hybrid-gulvsystem. Gulvsystemet består av en bjelkeramme av limtre overlagt med en 70 mm betongdekke. Den numeriske analysen er basert på resultatene av et fysisk eksperiment av bøyeoppførselen til et tre-betong hybrid-gulvsystem utsatt for en firepunkts bøyetest. Den eksperimentelle studien ble brukt til å vurdere nøyaktigheten av finittelementmetoden.

FEM-programvaren som ble brukt i denne numeriske analysen var ANSYS Mechanical APDL R2 2023. Den numeriske analysen av gulvsystemet var utfordrende på grunn av tre ortotropiske naturen og kravet på å beregne limtrebjelkenes mekaniske egenskaper.
FEA-analysen med ANSYS ga et lovende resultat, som nøyaktig matchet resultatet av det fysiske eksperimentet. Det nøyaktige resultatet av den numeriske analysen tillot en avansert undersøkelse, i form av tre parametriske studier. Effekten av, de forskjellige parameterne til gulvsystemet, på resultatet, ble analysert i disse parametriske studiene. Den første parametriske studien undersøkte påvirkning av "tykkelse av betongdekke" på maksimal forskyvning, Von Mises spenninger og de totale spenningene i kontaktelementet. På den andre siden, undersøkte den andre parametriske studien effekten av styrkeklassen av limtrebjelker, mens den tredje studien analyserte påvirkningen av lastplasseringen.

Resultatene av den parametriske analysen ga indikasjon på at tykkelsen på betongdekken er avgjørende effektiv på maksimal forskyvning og spenninger i tre-betong hybrid-gulvsystemer. Ved å øke tykkelsen på betongdekken med 20 mm, reduserte man maksimalt bøyning med 10 % og spenning med 14 %.
På den andre siden, å unngå konsentrerte laster i midtspennet og flytte lastene mot opplagerne, reduserte maksimal forskyvning med 29 % og spenningene med 33 %.
Videre arbeid som involverer effekten av "tykkelse til betongdekke" på naturlig frekvens og vibrasjon anbefales for avansert kunnskap om tre-betongkomposittgulvsystemer.

Contents

List of figures

List of tables

1 Introduction

1.1 Background

In the past 50 years the interest in timber-concrete composite structures (TCC) has grown enormously. In the beginning it was applicated as a refurbishment technique for old historical buildings in some of the European cities, such as Germany's Leipzig.(Holschemacher et al., 2002). In earlier years, the designed TCC floors did not meet the physical requirements of buildings with respect to fire resistance and sound insulation. The growing interest of timber-concrete composite systems resulted in a crucial development that led to the application of TCC systems in the construction of bridges. Several countries such as, The United States, New Zealand, Australia, Switzerland, Finland, Danmark, Sweeden and Norway, applicated TCC systems in upgrading exciting timber floors and constructing new buildings. (Natterer et al., 1996). One of the primary examples, is the construction of the Vihantaslami bridge in Finland in 1999. The TCC bridge spans 168 meters with a width of 11 meters. There are even earlier examples of timber-concrete composite bridges in the United States 1944, and the experimental bridge in New Zealand in 1957 (Yeoh et al., 2011).

The aim of this thesis is to advance the research on TCC systems, by conducting a finite element analysis, with ANSYS mechanical APDL 2023 R2, on a timber-concrete composite floor system. The presented finite element analysis (FEA) was executed on an experimental study of the flexural behavior of a TCC floor system, performed in the Laboratory of Composite Materials for Construction (LMC2) in the University Claude Bernard Lyon 1 (Ferrara et al., 2023).

The following Figure 1 illustrates the experiment on the timber-concrete composite floor system, linearly supported at two edges and subjected to a four-point bending test, in the middle of the span. The provided experimental results of the maximum displacement of the TCC floor system will be compared to the maximum displacement resulted in the finite element analysis (FEA). In addition, the stresses in the TCC floor system, due to the four-point bending test will be numerically investigated.
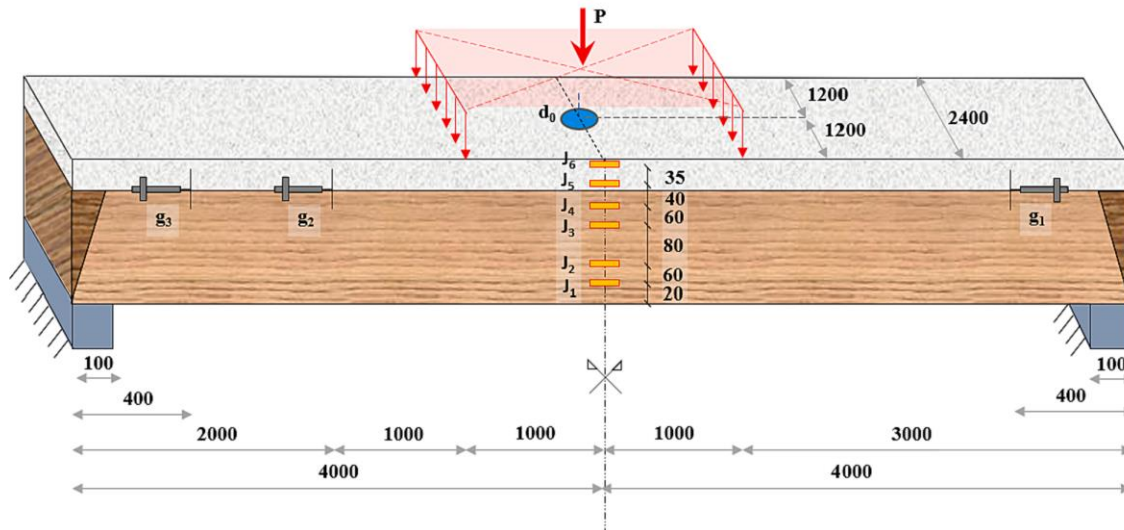
Figure 1 The set-up of the four-points bending test on the timber-concrete composite floor, applicated in the physical experiment in (LMC2) (Ferrara et al., 2023).

1.1.1 Timber-concrete composite structures TCC

Combining concrete with timber into a "Timber Concrete Composite" (TCC) has been a revolutionary concept in structural engineering in recent years. Connecting the concrete with the timber provides the advantages of both concrete and timber. The concrete as an overlaying part has compressive strength and acts in compression, while the underlying timber with a higher tensile strength and acts in tension. Using TCC as an alternative to pure concrete slab has many advantages, such as (Schänzlin & Dias, 2022):

- Reduction in dead load.
- Decreased CO2 emissions (Timber comes from wood, which is a natural, organic re-growing material)
- Lowered concrete's volume which results in faster constructing process and reduced need for transportation.
- The possibility of building higher buildings, as the dead load is reduced.

On the other hand, using timber-concrete composite TCC in comparison with using pure timber slab has the following advantages:

- Increasing the stiffness of the structure.
- Improving the load-bearing capacity.
- Improving the sound insulation.
- Reducing the vibrations.

Reports show that constructions with mass timber is 25% faster than similar constructions of on-site concrete. In addition, the requirements of construction traffic for mass timber are approximately 90% less than for concrete (Kremer & Symmons, 2015). Therefore, combining timber with concrete would give structural and serviceability performance advantages.

 The two components of TCC are usually connected with mechanical connectors such as self-tapping screws, notches or glued in plate. These mechanical connectors are illustrated if Figure 2, below (Mirdad et al., 2021).
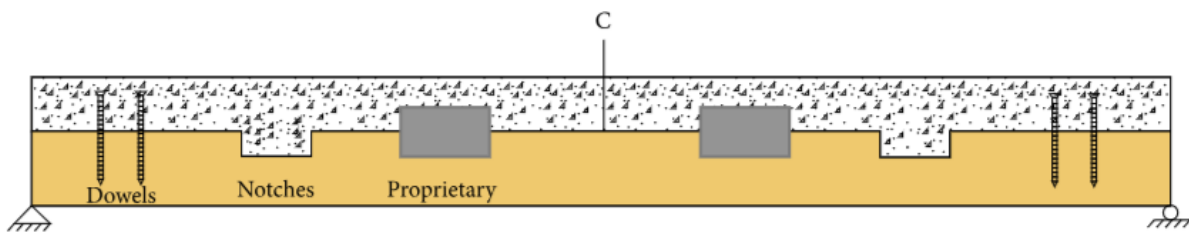
Figure 2 longitudinal section of a TCC system, and the type of mechanical connectors between timber and concrete (Mirdad et al., 2021).

1.1.2 Sustainability

Reducing energy use and CO2 emissions are of the main sustainability goals of the UN. In a global status report for buildings and construction, published by the UN in 2021, the magnificent increase of the demands of construction materials appeared throughout the recent two decades. From the year 2000 until 2015 steel and cement demands increased significantly. The following Figure 3, shows that the demand for steel for buildings construction rose from 230K tons to +500K tons, while the demand for cement increased from 900K tons to two million tons (UN, Environment Program, 2021).
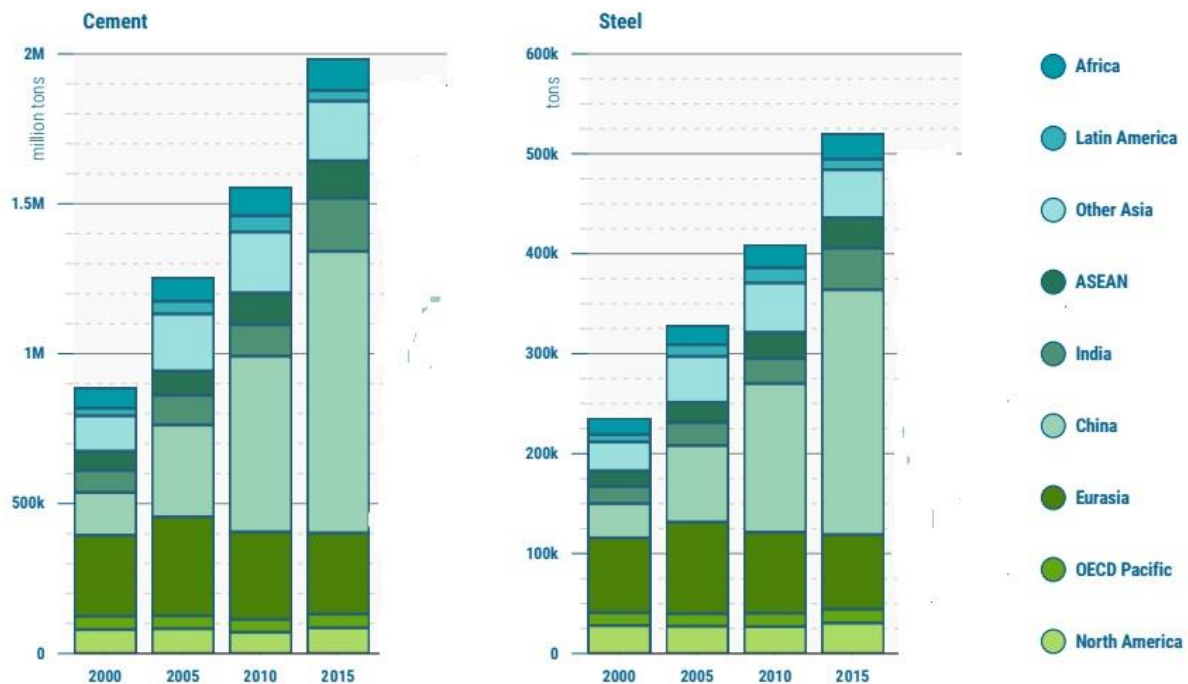
Figure 3 Demands of steel and cement for constructions between 2000-2015. (UN, EP, 2021).

The use of timber in multistorey buildings has increased throughout recent years. The consideration of timber as the primary structural material was inspired by the consciousness surrounding the sustainability of timber (Gosselin et al., 2017).

The importance of reducing CO2 emissions of buildings is a crucial goal. Therefore, it's critical today to use low-carbon materials to minimize the negative environmental impact of constructions (Pye et al., 2017).

Using timber-concrete composite (TCC) floor systems in multistorey buildings allows for an efficient structural impact, in terms of lightness, slenderness, and acoustic performance (Lamothe et al., 2021). In addition to achieving the crucial sustainability goal of the low environmental impact, due to the fact of that timber emits less carbon than steel and concrete (Plüss & Zwicky, 2014).

1.2 Aim

The finite element method (FEM) was developed over the years to meet the modern analysis requirements in structural engineering. The main contributor to the development of FEM, Ray William Clough stated in 1990 that the validation of the computational models will always be dependent on the physical experiments. This is one of the fundamental purposes of this thesis.

This thesis aims to provide the appropriate approach in conducting FEM-simulations, to achieve simulation's results close to the experimental results. In addition, it aims to offer an advanced analysis of timber-concrete composite structures, by conducting parametric studies on the physical experiment, and analyzing the influence of the different parameters in TCC systems on the results.

1.3 Limitations

This work will be an analysis of the flexural behavior of the timber-concrete composite floor system: taken from the physical experiment conducted in the University Claude Bernard Lyon. Other types of TCC structures will not be discussed in this thesis.

In addition, there are other limitations that will not be considered in this thesis. These limitations will be presented in the following points:

- The type of mechanical connections between timber and concrete.
- Post-failure behavior of the TCC floor system.
- The financial impact of TCC systems in comparison with other types of constructions.
- Vibration and natural frequency of TCC systems.

2 Theory

2.1 Timber as a construction material

Timber for construction is one of the most used buildings materials around the world, as it is used in both large and small buildings. Timber is considered as the only significant building material that does not have a harmful impact on the environment (Ramage et al., 2017).

Comparing the environmental impact of timber production with the many other materials timber competes with, has proven that timber's production results in less greenhouse gas emissions than concrete, steel, aluminum, and plastic. (Taylor, 2003)

The production of timber consumes less energy and sends out fewer pollutant to the environment. On the other hand, the manufacturing of steel and concrete is fewer energy efficient, emits more greenhouse gases, and release significantly more pollutant to the air and the water. (APA,2017). Many studies have been conducted in comparison between, the most used construction materials, and their environmental impact.

Figure 4 bellow shows results of one of these studies, where it shows the greenhouse gases emitted in the manufacture of building materials used in construction of single-storey housing in Sydney Australia. The results suggest that timber has, by far, the least emitted greenhouse gases among the other construction materials. (Australian Go, FWPRDC,2006)
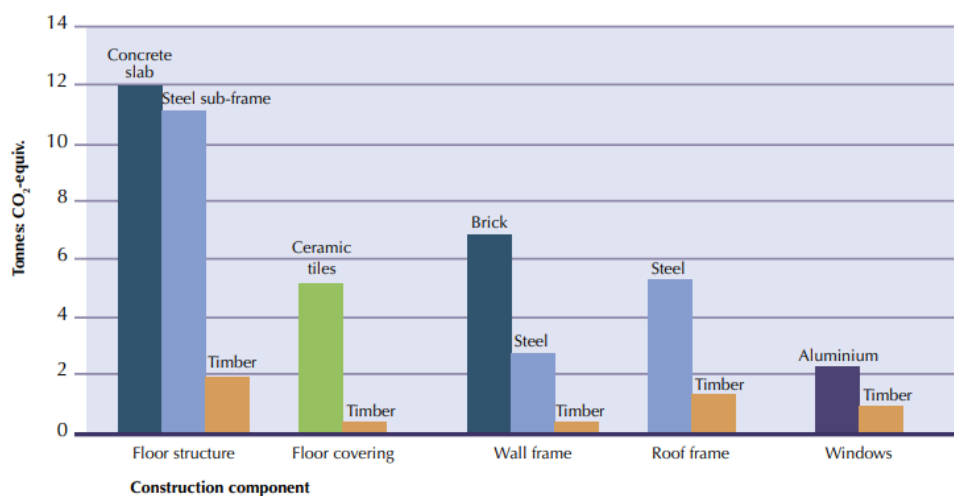
Figure 4 The emissions of greenhouse gases in the manufacture of building materials used in a range of constructions of single-storey houses in Sydney, Australia. (Australian GO. FWPRDC, 2006).

In addition, timber has several characteristics, which make timber a significant construction material. One of the most beneficial constructional characteristics of timber is that it has a high strength-to-weight ratio. Therefore, it is most efficient to use timber in constructions where it is carrying a lot of its self-weight. Timber can also have beneficial economic impact in constructions, as it is, on a large scale, factory prepared and brought to site for assembly. (Ramage et al., 2017).

Over the years, timber has been developed to reach the requirements of engineering timber. Several techniques have been conducted to produce timber with increased durability and strength. There are many products of structural such as, cross-laminated timber (CLT), mass timber, and glued laminated timber. Composite lumber, glulam and sandwich are considered as the most popular glued engineered timber products (Tsalkatidis, 2014).

However, in this thesis, glued laminated timber (glulam) is the one examined. Glulam is one of the most crucial products of timber as it has had a remarkable impact on modern architecture.

2.1.1 Glued laminated timber

Glued laminated timber (Glulam) believed to be first used in the early 1860s in the building of the hall of king Edward college in Southampton (Lehringer & Gabriel, 2014). While other sources suggest that it was first invented in 1890s and later patented in 1901 in Switzerland.

 Since then, glulam has been used on a large scale, especially in the Nordic countries. Glulam consists of multiple layers of lamellar packed on each other's and glued together. Glulam has been revolutionary in dimensions and length of timber, as timber depends on the length of the tree (Ong, 2015). Some manufacturers of timber structure deliver glulam beams with a maximum length of up to 36 meters, while trusses can be even longer (Arcwood, 2000).

The individual components of glulam (Lamellae) are glued over the entire contact surface with adhesives. The development of synthetic resin adhesives to be waterproof and mildew-proof has made glulam a significant material in the construction world. It has allowed for larger cross-sections and made glulam greater in significancy as a load-bearing constructional material.

Figure 5 Glued laminated timber (Glulam) (Balb & Sandhaas, 2017)

2.1.2 BS EN 14080:2013

EN 14080 is a European standard which sets the performance requirements of the following glued laminated timber products:

- Glulam.
- Glulam with large finger joints; with minimum finger's length of 45 mm.
- Glued solid timber.
- Block-glued glulam.

This standard also includes the requirements of glulam products that are treated against biological attacks, but it does not include products treated with fire retardants.

In addition, it differentiates horizontal laminated glulam with one or more adjacent lamellae from the multiple glulam members which are glued to form a single wider member (Block-glued glulam). Figure 6 illustrates these several types of glulam.
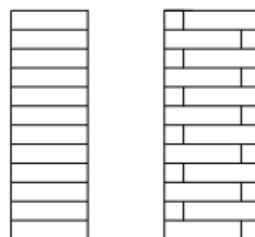
Figure 6 Horizontal glued laminated timber with one adjacent lamellae (left) VS multiple adjacent lamellae (right) (Balb, Sandhaas, 2017).

EN 14080 lists details of both strength classes and production requirements. It sets out a new generational European standard as it unifies several standards and can replace standards such as EN 385 – EN 387, EN 390 – EN 392, EN 1194 and EN 391 (European Standards, 2013)

2.1.3 Properties of structural timber

Wood is a natural and organic material, therefore there are variations in its properties, even among samples of same species (Ramage et al., 2017).

To determine the properties of timber, classification of the strength of timber is needed according to EN338 (Norwegian standard, 2016). The most structural timber used in Norway is of the grade C24, while the highest strength class produced is C30.

Most studies on the properties of timber conducted in Norway have reported an average of modulus of elasticity MOE over 11500 N/mm^2, and an average of modulus of rupture over 42 N/mm^2. While the average of density reported in these studies are higher than 400 kg/cm^3. The results reported from the studies on timber done in Norway are presented in Table 1 below (Fischer, 2016).

Table 1. Studies conducted in Norway on the properties of timber (Fischer, 2016).

Study		Year	N	MC (%)	Density(kg/cm^3)	MOE(N/mm^2)	MOR(N/mm^2)
Vestøl et al.		2012	333	12	442	12900	50.9
Haartveit and Flæte		2002	144	12	434	12400	45.3
Eikenes et al.		1996	105	12	-	11400	42.0
Høibø		1991	141	12	395	10100	31.4
Eikenes		1991	630	12	330	10000	33.2
Fosile and Moen		1968	1351	15	470	12700	49.6

Characteristic strength and stiffness properties of homogeneous glued laminated timber, according to EN 14080:2013, are presented in Table 2 (Blab & Sandhaas, 2017).

.

Table 2 Characteristic strength and stiffness properties of homogeneous glued laminated timber (Balb & Sandhaas, 2017).

N/mm²	GL20h	GL22h	GL24h	GL26h	GL28h	GL30h	GL32h
$f_{m,g,k}$	20	22	24	26	28	30	32
$f_{t,0,g,k}$	16	17.6	19.2	20.8	22.3	24	25.6
$f_{t,90,g,k}$				0.5			
$f_{c,0,g,k}$	20	22	24	26	28	30	32
$f_{c,90,g,k}$				2.5			
$f_{v,g,k}$				3.5			
$f_{r,g,k}$				1.2			
$E_{0,g,mean}$	8400	10500	11500	12100	12600	13600	14200
$E_{0,g,05}$	7000	8800	9600	10100	10500	11300	11800
$E_{90,g,mean}$				300			
$E_{90,g,05}$				250			
$G_{g,mean}$				650			
$G_{g,05}$				540			
$G_{r,g,mean}$				65			
$G_{r,g,05}$				54			
kg/m³							
$\rho_{g,k}$	340	370	385	405	425	430	440
$\rho_{g,mean}$	370	410	420	445	460	480	490

2.1.4 Orthotropic nature of timber

Timber is considered an orthotropic material. It has independent and unique mechanical properties in the direction of three perpendicular axes.

- The longitudinal axis (L), which is parallel to the grain (fiber).
- The radial axis (R) is perpendicular to the grain in the radial direction, which is normal to the growth rings.
- The tangential axis (T) is tangent to the growth rings, while perpendicular to the grain.

The three principal axes of timber with respect to growth rings and grain direction are presented in Figure 7 that is shown below (Forest Products Laboratory, 2010).
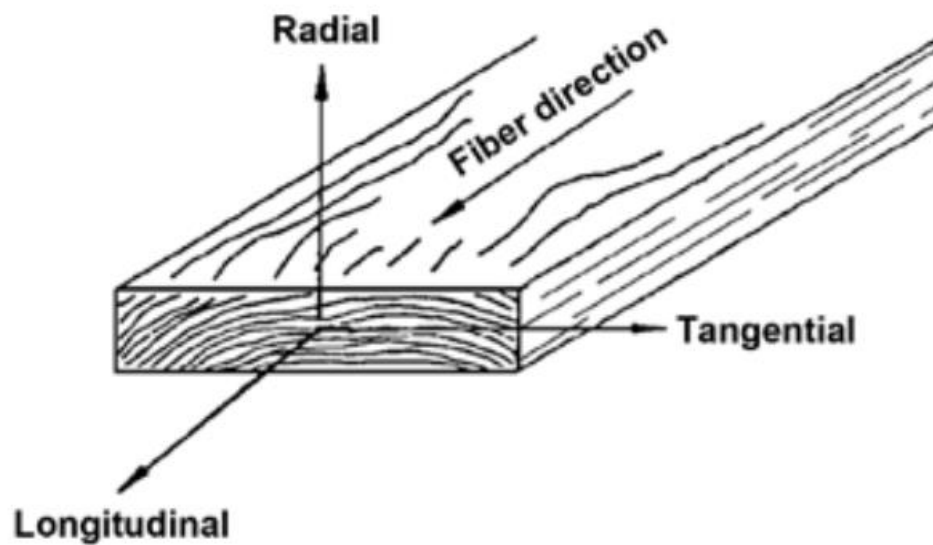
Figure 7 The three principal timber's axes with respect to growth rings and grain direction (Forest production . Laboratory, 2010).

2.1.5 Elastic properties

To describe the elastic behavior of timber: twelve constants are required, while nine of them are independent. These constants will be presented in the following points:

- Three moduli of elasticity E_L, E_R and E_T (E_{XY}, E_{YZ}, E_{XZ}).
- Three moduli of rigidity G (G_{XY}, G_{YZ}, G_{XZ})
- Six Poisson's ratio μ.

Both the Poisson's ratio μ and moduli of elasticity E are related as shown in equation 1.2 (Forest Products Laboratory, 2010).

$$\frac{\mu ij}{Ei} = \frac{\mu ji}{Ej} \, , \, i \neq j \quad i,j = L,R,T \qquad (1)$$

 L: longitudinal axis, R: radial axis & T: tangential axis.

2.1.6 Modulus of elasticity

Elasticity of the material indicates that the deformation caused by low stress is completely recoverable once the load is removed. While the plastic deformation or failure occurs when

higher levels of stress are applied. Timber has three moduli of elasticity along the three axes. E_L along the longitudinal axis, E_R along the radial and E_T along the tangential axis.

To obtain the values of these three moduli, a compression tests are required. However, it is suggested that the data for E_R and E_T are not extensive. In addition, there are several factors which can influence the values of the elastic constants: resulting variations within same species. Such as the moisture content the specific gravity.

The modulus of elasticity E_L is determined by applying bending tests (Forest Products Laboratory, 2010).

MOE and MOR testing occurs by using a machine to apply a four-points bending test as shown in the following Figure 8.

Figure 8 Machine from Instron 5800 applying four-points bending tests for the identifications of MOE and MOR. (Fischer, 2016).

2.1.7 Poisson's Ratio

When applying an axial load on a member, the deformation perpendicular to the load's direction is proportional to the parallel deformation to the load's direction. The Poisson's ratio is the ratio of the transverse to the axial strain. There are six Poisson's ratios, which are referred to as following:

1. μ_{LR}, where L refers to the direction of the applied stress, while R gives the direction of the lateral deformation.
2. μ_{RL}, the applied stress is in the radial axis, while the lateral deformation is in the longitudinal.
3. μ_{LT}, stressed in the longitudinal axis and the lateral deformation in the tangential.
4. μ_{TL}. The deformation is in the longitudinal axis caused by tangential stress.
5. μ_{RT}. The deformation is in the tangential axis caused by stress applied in the radial axis.
6. μ_{TR}. The deformation is in the radial axis resulted by stress applied in the tangential.

Table 3 shows average values of Poisson's ratios determined by conducting experiments on a few species of hardwood (Forest Products Laboratory, 2010).

Table 3. Average Poisson's ratios for various species of wood with approximately 12 % moisture content.

Species	μ_{LR}	μ_{LT}	μ_{RT}	μ_{TR}	μ_{RL}	μ_{TL}
Baldcypress	0.338	0.326	0.411	0.356	—	—
Cedar, northern white	0.337	0.340	0.458	0.345	—	—
Cedar, western red	0.378	0.296	0.484	0.403	—	—
Douglas-fir	0.292	0.449	0.390	0.374	0.036	0.029
Fir, subalpine	0.341	0.332	0.437	0.336	—	—
Hemlock, western	0.485	0.423	0.442	0.382	—	—
Larch, western	0.355	0.276	0.389	0.352	—	—
Pine						
Loblolly	0.328	0.292	0.382	0.362	—	—
Lodgepole	0.316	0.347	0.469	0.381	—	—
Longleaf	0.332	0.365	0.384	0.342	—	—
Pond	0.280	0.364	0.389	0.320	—	—
Ponderosa	0.337	0.400	0.426	0.359	—	—
Red	0.347	0.315	0.408	0.308	—	—
Slash	0.392	0.444	0.447	0.387	—	—
Sugar	0.356	0.349	0.428	0.358	—	—
Western white	0.329	0.344	0.410	0.334	—	—
Redwood	0.360	0.346	0.373	0.400	—	—
Spruce, Sitka	0.372	0.467	0.435	0.245	0.040	0.025
Spruce, Engelmann	0.422	0.462	0.530	0.255	0.083	0.058

2.1.8 Modulus of rigidity

The resistance to the deflection caused by shear stresses on a member, is called modulus of rigidity or shear modulus. As in the modulus of elasticity, modulus of rigidity varies within and between same species of wood, and it is dependent on the moisture content alongside the specific gravity.

Shear moduli are referred to as G_{LR}, G_{LT} and G_{RT}, and are explained as following *(*Forest Products Laboratory*, 2010):*

- G_{LR}: modulus of rigidity based on shear strain in the LR plane and shear stresses in LT and RT.
- G_{LT}: modulus of rigidity based on shear strain in the LT plane and shear stresses in LR and RT.
- G_{RT}: modulus of rigidity based on shear strain in the RT plane and shear stresses in LR and LT.

2.1.9 Oriented strand board

Oriented strand board (OSB) is a panel made of thin strands of wood glued together by using water-resistant resin (Yuan et al., 2021). It is manufactured by hot-pressing slender wood strands, forming three layers crossing at right angle. The two external layers (upper & lower) consist of strands oriented along the panel's major axis, while the strands in the core-layer are at 90° to that axis (Plenzler et al., 2017).

Several experiments were conducted to determine OSB's material properties, where the results suggested that OSB-board is of an orthotropic nature (Zhu et al., 2005).

OSB are used in construction on a large scale, applicated in walls, roofs, and floors (Yuan et al., 2021).

According to NS-EN 300 OSB-boards are classified is four groups (OSB/1, OSB/2, OSB/3, and OSB/4), where OSB/3 and OSB/4 are classified as load-bearing boards for humid conditions. OSB/3 is considered to have an under-floor as an application area (SINTEF Building Research Design Guides, 2021).

Some of the mechanical properties of OSB/3, according to NS-EN 12369-1, are presented in Table 4.

Table 4 Some of the characteristic values of OSB/3 according to NS-EN12369-1(SINTEF, 2021)

OSB/3	Thickness (mm)	Density (Kg/m^3)	Bending strength(N/mm$^{2)}$)		Modulus of elasticity (N/mm^2)	
			$f_{m,0}$	$f_{m,90}$	$E_{m,0}$	$E_{m,90}$
	> 18-25	550	14,8	7,4	4930	1980

2.1.10 Calculations of the mechanical properties of orthotropic materials

The orthotropic elastic material has three orthogonal symmetrical planes. However, the compliance anisotropic matrix of elasticity can be simplified to have 9 independent constants instead of 21 (Wickeler & Naguib, 2020).

$$\begin{Bmatrix} \varepsilon_1 \\ \varepsilon_2 \\ \varepsilon_3 \\ \varepsilon_4 \\ \varepsilon_5 \\ \varepsilon_6 \end{Bmatrix} = \begin{bmatrix} \dfrac{1}{E_x} & \dfrac{-v_{yx}}{E_y} & \dfrac{-v_{zx}}{E_z} & 0 & 0 & 0 \\ \dfrac{-v_{xy}}{E_x} & \dfrac{1}{E_y} & \dfrac{-v_{zy}}{E_z} & 0 & 0 & 0 \\ \dfrac{-v_{xz}}{E_x} & \dfrac{-v_{yx}}{E_y} & \dfrac{1}{E_z} & 0 & 0 & 0 \\ 0 & 0 & 0 & \dfrac{1}{2G_{yz}} & 0 & 0 \\ 0 & 0 & 0 & 0 & \dfrac{1}{2G_{zx}} & 0 \\ 0 & 0 & 0 & 0 & 0 & \dfrac{1}{2G_{xy}} \end{bmatrix} \begin{Bmatrix} \sigma_1 \\ \sigma_2 \\ \sigma_3 \\ \sigma_4 \\ \sigma_5 \\ \sigma_6 \end{Bmatrix}$$

Figure 9 The compliance anisotropic matrix of elasticity (Wickeler & Naguid, 2020).

When a material is evaluated as an orthotropic material the calculations of the mechanical properties happen as following:

- Moduli of elasticity (E_{XY}, E_{YZ}, E_{XZ})

$$E = \frac{stress}{strain} = \frac{\sigma}{\varepsilon} \qquad (2)$$

It must be taken into consideration stresses and strains in the longitudinal and transverse directions.

- **Poisson's ratio (μ_{XY}, μ_{YZ}, μ_{XZ})**

$$\mu_{XY} = -\frac{\varepsilon_Y}{\varepsilon_X} \qquad (3)$$

ε_Y: strain in y-direction, ε_X: strain in x-direction.

- **Moduli of rigidity (shear modulus)**
  Shear modulus for orthotropic materials can be obtained in three ways (Ashkenazi, 1978):

$$G_{XY} = \frac{E_{XZ}}{2(1+\mu_{XZ})} \qquad (4)$$

$$G_{XY} = \frac{\sin\theta^2 \times \cos\theta^2}{\frac{1}{E_{XZ}} - \frac{\cos\theta^4}{E_{XY}} - \frac{\sin\theta^4}{E_{YZ}} + \frac{2\mu_{XY}}{E_{XY}} \times \sin\theta^2 \times \cos\theta^2} \qquad (5)$$

$$G_{XY} = \frac{\sin\theta^2 \times \cos\theta^2}{\frac{1}{E_{XZ}} - \frac{\cos\theta^4}{E_{XY}} - \frac{\sin\theta^4}{E_{YZ}} + \frac{2\mu_{YZ}}{E_{YZ}} \times \sin\theta^2 \times \cos\theta^2} \qquad (6)$$

(E_{XY}, E_{YZ}, E_{XZ}) moduli of elasticity at θ rotation with respect to the major considered axis.

2.2 Concrete

Concrete is one of the oldest building materials. It has been used in construction since the roman times. Back then it consisted of aggregates such as rocks, bricks, or ceramic tiles bonded with gypsum and quicklime. It also contained volcanic dust called Pozzolana to resist salt water. (Delatte, 2001). Throughout the years concrete has been developed extensively, especially in the 20th century, to reach the necessary construction requirements. Figure 10 shows the development of the compressive strength of concrete from the start of the 20th century until the early 90s (Spasojevic, 2008).
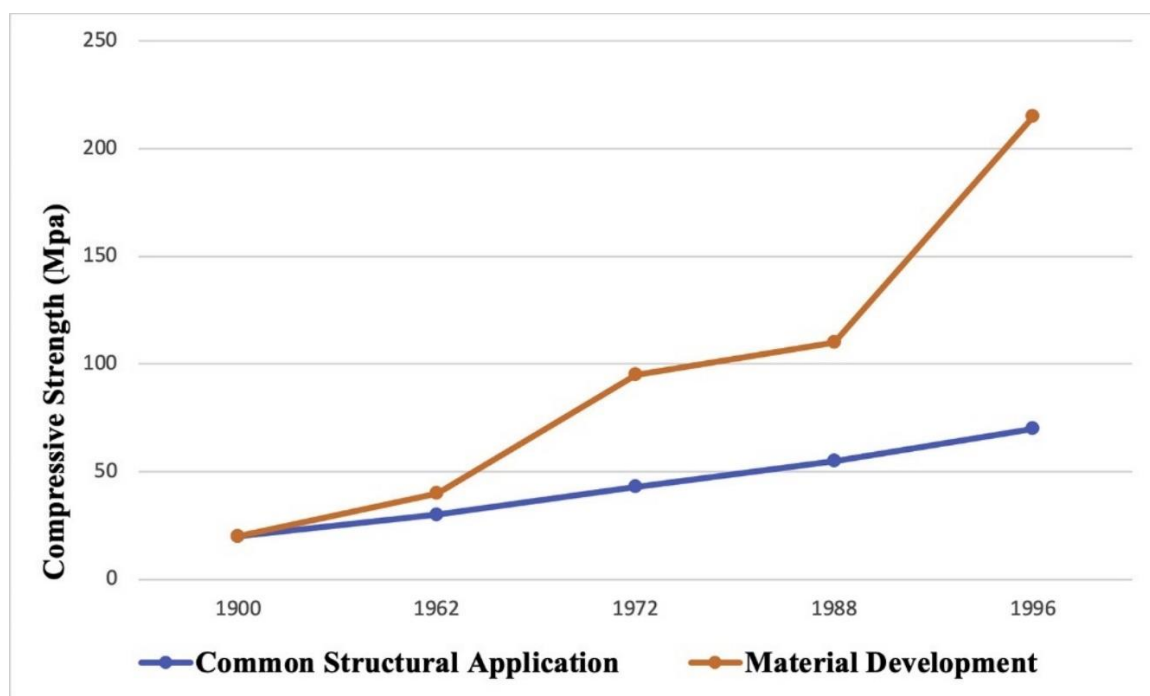
Figure 10 The development of the compressive strength of concrete between 1900-1996, and the common application of concrete, (Spasojevic, 2008).

The compressive strength of concrete was achieved through carefully selecting the right aggregates and decreasing the water's ratio to binder material. The invention of water-reducing admixtures allowed for the significant reduction of water content (Tennis et al., 2004). All these factors allowed for the creation of what is called: ultra-high-performance concrete (UHPC), which has a compressive strength of +200 MPa (Bajaber & Hakeem, 2021). The basic components of UHPC are presented in Figure 11.
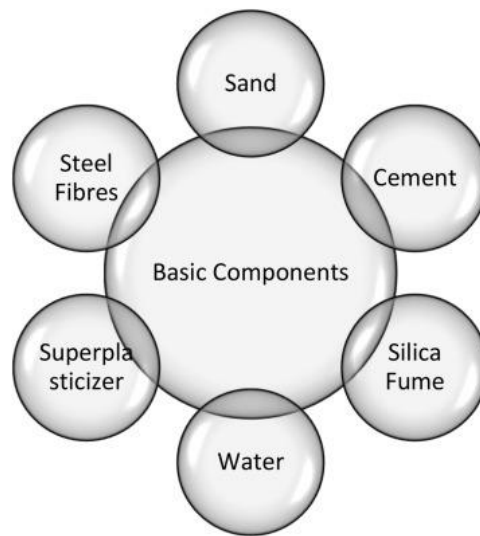
Figure 11 The basic components of ultra-high-performance concrete, (Bajaber & Hakeem, 2021).

The following Figure 12 shows the optimum proportions for the mixture of 1m^3 of UHPC, where it is suggested that the water makes 6.56 %.
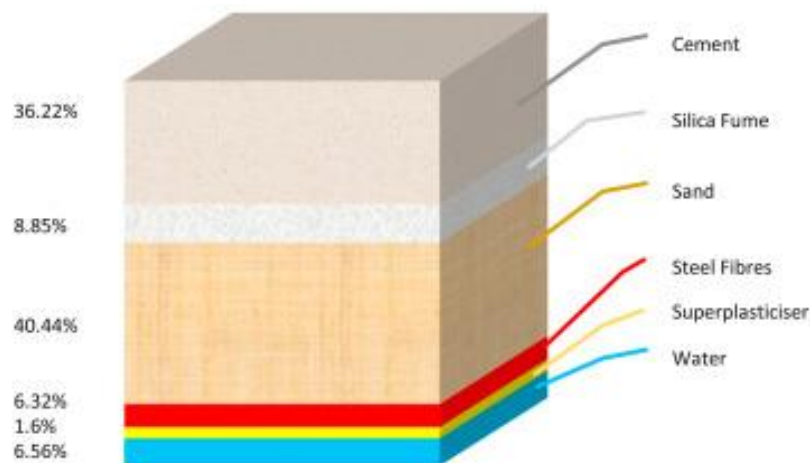
Figure 12 proportions of the mixture of one cubic meter of ultra-high-performance concrete, according to (Bajaber & Hakeem, 2021).

2.2.1 The compressive strength of concrete

The compressive strength of concrete indicates the performance of the structures during service life. It is commonly determined through compressive strength tests of hardened concrete. It is also necessary to re-test the compressive strength of the hardened concrete to ensure supervisory. The traditional most common method of testing is to core the concrete structure. (Khormani & Jaari, 2023)

However, it is a destructive method as it decreases the structural member's cross-section (Landis & Bolander, 2009). Therefore, new non/destructive methods of compressive-strength testing (NDT) have been invented, such as The Schmidt hammer, the Windsor probe, and the ultrasonic pulse velocity test. These methods have contributed to the achievement of faster and accurate compressive-strength testing. (Nepomuceno & Bernardo, 2019).

The compressive strength is calculated according to NS-EN 1992-1-1.

2.2.2 Modulus of elasticity of concrete

Modulus of elasticity of concrete E_C is the ratio between the normal stress to the normal strain. It has a crucial influence on the lateral deflection of a reinforced-concrete structure. It is one of the mechanical properties of a linear elastic solid materials. The elasticity describes the ability of the material to return to its original shape after removing the loads. The modulus of elasticity of concrete is influenced by several parameters such as the compressive strength, the age, the type of aggregates used, cement's type, and the rate of the load. The modulus of elasticity, which is also referred to as Young's modulus, describes the relative stiffness of the material and can be calculated, according to EN1992-1-1, as following (Asiri & Mohammad, 2018):

$$E = \frac{Stress}{Strain} \qquad (7)$$

$$Stress = \sigma = \frac{F}{A} \qquad (8)$$

$$Strain = \varepsilon = \frac{\Delta L}{L} \qquad (9)$$

$$; F = force, A = sectional\ area\ , \Delta L = change\ in\ length, L = initial\ length$$

NS-EN 1991 (Eurocode 1) and NS-EN 1992 (Eurocode 2) have been the replacement for the Norwegian standards NS 3473, NS EN 206-1, NS 3465 and NS 3420 since 2010 and the cover the following:

NS-EN 1991 includes the following parts:

- ➢
  - 1-1: Specific gravity and payloads
  - 1-2: Loads in case of fire.
  - 1-3: Snow loader
  - 1-4: Wind loader
  - 1-5: Thermal influences
  - 1-6: Loading during execution.
  - 1-7: Accident loads
- ➢ 2: Traffic load on bridges
- ➢ 3: Loads from cranes and machinery
- ➢ 4: Silos and containers

NS-EN 1992 has the following parts:

- ➢
  - 1-1: General rules and regulations for buildings
  - 1-2: Fire technical dimensioning
- ➢ 2: Bridges
- ➢ 3: Silos and containers
- ➢ 4: Design of anchors in concrete

2.2.3 The design values of concrete properties according to EN 1992-1-1

According to the Norwegian standard NS 3473 (which was replaced, in 2010, by EN1992) the relationship between the modulus of elasticity and the compressive strength is as following (Ahmadi & Kioumarsi, 2023):

$$E = 9500(f')^{0'3} \qquad\qquad (\mathbf{10})$$

- f' or f_{CK} is the **characteristic compressive strength** of concrete and can be determined as the first value in the concrete's class designation, for example f_{CK}= 35 MPa for C35/45 concrete.

- **Mean compressive strength** f_{Cm} is related to the characteristic compressive strength f_{CK} as following:

$$f_{Cm} = f_{CK} + 8\text{MPa} \qquad (11)$$

- **Design compressive strength** f_{Cd}

$$f_{Cd} = a_{cc} . f_{CK} / \gamma_C \qquad (12)$$

Where γ_C is the partial safety factor of concrete according to EN1992-1-1 §2.4.2.4

While a_{cc} is a coefficient that considers the long-term effects on the compressive strength.

- **Modulus of elasticity** E_{cm}

$$E_{cm} \text{ [MPa]} = 22000 \cdot (f_{cm} / 10\text{MPa})^{0.3} \qquad (13)$$

f_{cm} : Mean compressive strength.

- **Poisson's ratio** μ

Poisson's ratio is one of the most crucial elastic parameters for both the theoretical and numerical analysis. It was named after Siméon Denis Poisson (1781–1840), and it describes the ratio of the absolute value of both the lateral and the axial strains when the material is under tension or compression. (Dong et al., 2021).

The values of Poisson's ratio for cementitious materials vary from 0.15 to 0.3 (Wang, 2004), and they depend on whether the loads are dynamic or static.

According to EN1992-1-1 §3.1.3(4) Poisson's ratio has a value of:

- ✓ μ = 0.2 for uncracked concrete.
- ✓ μ = 0.0 for cracked concrete.

  Figure 13 shows the stress-strain diagram for concrete in compression, according to Eurocode 2.
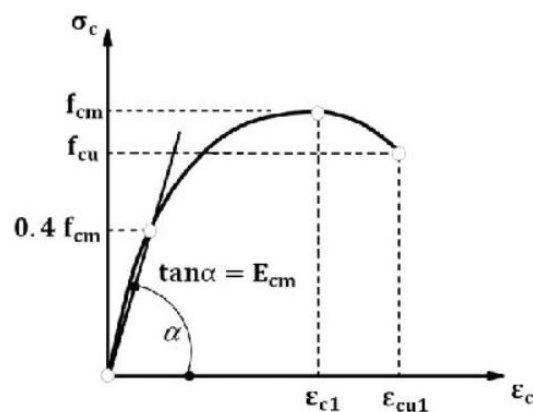
Figure 13 Stress-strain curve for concrete, according to EC2.

- **Modulus of rigidity** G

Modulus of rigidity or the shear modulus for concrete G is described in EN1992-1-1 §3.1 by the following equation 14:

$$G = E / [2 \cdot (1 + \mu)] \qquad (14)$$

E: Modulus of elasticity

μ: Poisson's ratio.

- **Density of concrete** ρ

The density of concrete is one of the most crucial mechanical properties. It has a major influence on the compressive strength and depends on the cement content (Zhang et al., 2016).

According to EN 1992-1-1§3.1: the density of reinforced concrete is:

$$\rho \approx 2500 \; Kg/m^3 \qquad (15)$$

The European standard for concrete describes the design properties for concrete with respect to the several different strength classes of concrete, starting from the lowest strength class C12/15 up until C90/105.

The following Table 5 shows concrete design properties according to EN1992-1-1 for (γ_c = 1.50, f_{yk} = 500 MPa) for the strength classes between C35/45 – C70/85, as the examined strength class in this thesis is C40/50.

Table 5 The design properties of concrete according to EN1992-1-1 for y_c=1.5 and f_{yk} = 500MPa.

Symbol	Description	C35/45	C40/50	C45/55	C50/60	C55/67	C60/75	C70/85
f_{ck} (MPa)	Characteristic cylinder compressive strength	35	40	45	50	55	60	70
$f_{ck,cube}$ (MPa)	Characteristic cube compressive strength	45	50	55	60	67	75	85
f_{cm} (MPa)	Mean cylinder compressive strength	43	48	53	58	63	68	78
f_{ctm} (MPa)	Mean tensile strength	3.21	3.51	3.80	4.07	4.21	4.35	4.61
E_{cm} (MPa)	Elastic modulus	34077	35220	36283	37278	38214	39100	40743
f_{cd} (MPa) (for α_{cc}=1.00)	Design compressive strength (for α_{cc}=1.00)	23.33	26.67	30.00	33.33	36.67	40.00	46.67
f_{cd} (MPa) (for α_{cc}=0.85)	Design compressive strength (for α_{cc}=0.85)	19.83	22.67	25.50	28.33	31.17	34.00	39.67
f_{ctd} (MPa) (for α_{ct}=1.00)	Design tensile strength (for α_{ct}=1.00)	1.50	1.64	1.77	1.90	1.97	2.03	2.15
ρ_{min} (%)	Minimum longitudinal tension reinforcement ratio	0.167	0.182	0.197	0.212	0.219	0.226	0.240
$\rho_{w,min}$ (%)	Minimum shear reinforcement ratio	0.095	0.101	0.107	0.113	0.119	0.124	0.134

3 Methodology

3.1 Finite element method

The finite element method (FEM), as a concept, was first coined by Ray William Clough in an article in 1960 (Pradhan & Chakraverty, 2019). However, the significant development of the method started a few years earlier. It was when Clough went to Norges Tekniske Hogskole in Trondheim, Norway in September 1956. While he was in Norway, he became aware of the crucial work that had been done by Dr John Argyris in the field of airplane structural analysis. Several articles that were published by Butterworths of London as a single volume with the title 'Energy Theorems and Structural Analysis.' In 1960 Clough established the name FEM in the paper he gave at the ASCE Conference on Electronic Computation in Pittsburgh (Clough, 2004).

FEM is one of the most used methods and has a wide application in all computational areas of physics and engineering. It is certainly the most flexible and can be adapted to a wide range of numerical investigations. This computational technique has allowed to obtain approximate solutions to several engineering's boundary value problems. It has simplified the engineering's problems throughout dividing the system into elements and finding individual solutions that fulfill the differential equation within the boundary of that system (Rapp, 2022). These elements (subdomains) are what are known as finite elements (FEs). FEM is used to solve complex mathematical problems that are too complicated to solve without errors.

A finite element analysis (FEA) has a wide range of applications, such as analyzing structures, models, fatigues, heat transfer, flow simulations, fluid structural interactions and failure diagnoses. As for the structural analysis, FEM determines the displacement and stress under a statical loading conditions. The conducted analysis can be either linear or nonlinear, where the linear analysis assumes that the material has an elastic region behavior without plastic deformation. While the nonlinear involves plastic deformation (Bi, 2017).

The finite element analysis (FEA) has several advantages that can be summed up in the following points (Bi, 2017):

- FEA is insensitive to complex geometries.
- The ability of analyzing a wide range of engineering problems (solid mechanism, Fluid flows, heat problems, electrostatics, and dynamics)
- The capability of handling complex boundary conditions such as solid mechanics over constraints.

- FEA can manage complex load conditions such as distributed loads and time-dependent loads.

The divide and conquer strategies during the modelling procedure is applied to obtain simple unites, as was called previously elements or subdomains. These elements are assembled with each other through interconnection points. These points are called nodes. Within the system, each element is related to a set of nodes, and the behavior of the element is model-dependent on the behavior of the nodes. This technique of dividing a continuous problem (a domain) into a finite number of elements is called discretization. The discretization process is also referred to as meshing process. Figure 14 explains the discretization of a continuous domain into elements and nodes. (Bi, 2017).
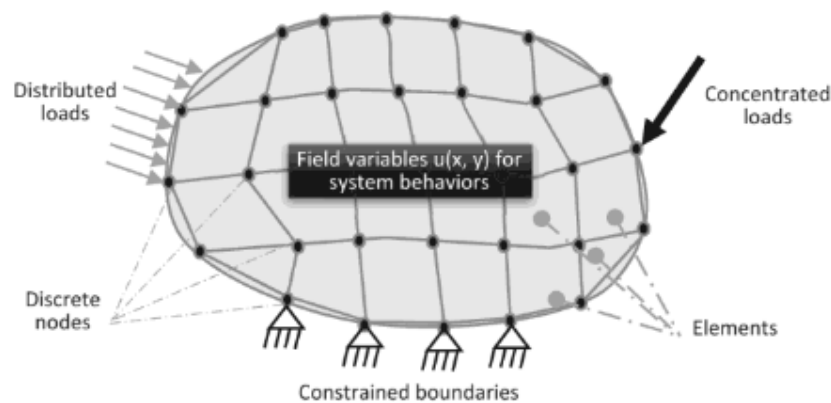
Figure 14 The discretization of a continuous domain into nodes and elements (Meshing), (Bi, 2017).

Each of these nodes has a limited number of degrees of freedom (DOFs) and the number of DOFs depends on the chosen element type in the finite element analysis (FEA).

There are several engineering softwires (FEM-software) that can run finite element analysis (FEAs). ANSYS Student 2023 R2 was chosen for this thesis. ANSYS-Student has a limited number of nodes allowed; however, it offers a free student-license.

3.1.1 Procedure of Finite Element Analysis in ANSYS

In any finite element analysis, there are 10 steps to make in, at least, three different processors. These processors are (PREP7), (SOL) and (POST1 or POST26). These steps will be presented as following (Thompson & Thompson, 2017).

/PREP7

1. Defining the geometry of the solid model.
2. Selecting the Element Types.
3. Defining the properties of the materials.
4. Meshing.

/SOLUTION

5. The definition of the boundary conditions.
6. Defining the loads.
7. Setting the option of the solution.
8. Solving.

/POST1 or POST26
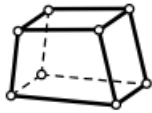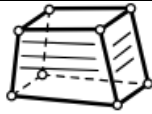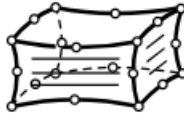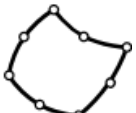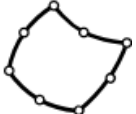
9. Plotting and viewing the results.
10. Verifying and comparing the results

The library of ANSYS contains many diverse types of elements, where each one has its unique set of characteristics. An element can be presented as one single point (node), as for an example to define a mass element. On the other hand, an element can be a complicated solid with an enormous number of nodes. One of the most crucial steps in executing a FEA, is to select the right type of element. The selected element type must be able to depict the problem's behavior, while making the computational process as simple as possible. The complexity and the time needed for FEAs is significantly dependent on the accurate selection of the element type. Element shape characteristics can be summed up in the following points (ANSYS, Inc, 2011):

- A point element, which is defined by one node. Example, mass element.

- A line element which can be presented as a line/arc that connects two or three nodes. This can be for modeling beams, truss elements, columns, pipes, and axisymmetric shells.

- An area element, which can have a rectangular shape or quadrilateral and is typically used for 2-D solid elements or shell elements.

- A volume element with a tetrahedral or brick shape, which is typically used as a 3-D solid element.

There is also the possibility of creating a user-defined by using the command Creating New Element. Inside the ANSYS's library there are many diverse types of elements. Some of the most relevant types of elements to this thesis are presented in the following Table 6.

Table 6 some of the element types inside the library of ANSYS. (ANSYS, Inc, 2011).

Element type	Nodes	Degree of freedom (DOFs)	Shape
BEAM161 Explicit 3-D Beam	**3** nodes	**11 DOFs** (UX, UY, UZ, ROTX, ROTY, ROTZ, VX, VY, AX, AY, AZ)	
SHELL181 Structural Shell 3-D	**4** nodes	**6 DOFs** (UX, UY, UZ, ROTX, ROTY, ROTZ)	
SOLID65 Reinforced concrete structural Solid 3-D	**8** nodes	**3 DOFs** (UX, UY, UZ)	
SOLID185 Structural Solid 3-D	**8** nodes	**3 DOFs** (UX, UY, UZ)	
SOLID186 Structural Solid 3-D	**20** nodes	**3 DOFs** (UX, UY, UZ)	
MESH200 Meshing Facet 2-D/3-D	**2-20** nodes	**None**	
CONTA174 Surface-to-Surface contact 3-D	**8** nodes	**10 DOFs** (UX, UY, UZ, TEMP, TTOP, TBOT, VOLT, MAG, PRES, CONC)	
TARGE170 Contact Target Segment 3-D	**8** nodes	**10 DOFs** (UX, UY, UZ, TEMP, TTOP, TBOT, VOLT, MAG, PRES, CONC)	

By selecting the analysis type, design variables and the defining of the mathematical model with governing differential equations, the mathematical model gets converted into element models. FEM uses approximation methods such as Direct stiffness methods, weighted residual methods, or minimum potential energy methods (Bi, 2017)

3.1.2 Application of Finite Element Method

- **Direct stiffness method**

The direct stiffness method is one of the methods used in the application of FEM. It is also referred to as the deflection method, or the matrix stiffness method. It depends on the relationship between force, stiffness, and deflection. It is one of the most applicated methods in executing structural analysis. The name "Deflection method" describes the main aim of the stiffness method. Therefor it is one of the most common methods in the calculations of the displacement of an element. The material's stiffness is a major factor and can be identified by obtaining its shape, size, and properties. The equation (16) illustrates the relationship between force, stiffness, and displacement. By knowing the force and the stiffness, the displacement can be obtained. Once the displacement is known, the calculation of the stresses and strains.

Equilibrium equation for rods (Cook, 2007):

$$[k]\{d\} = \{r\} \qquad\qquad (16)$$

Where:

- $[k]$ is the stiffness matrix.
- $\{d\}$ is the displacement victor.
- $\{r\}$ is the force's victor.
- $[k], \{d\}, \{r\})$ for element's equilibrium while $([K], \{D\}, \{R\})$ for system's equilibrium.

The computation of member stiffness matrix locally and globally then throughout assembly the global stiffness matrix for the entire structure can be obtained (Papadrakakis & Sapountzakis, 2017).

The direct stiffness method depends on the principle of that, the nodal forces and displacement, for any structure in equilibrium, must be continuous and compatible in both the individual finite element and the whole structure (Ellobody et al., 2013).

- **Method of weighted residuals**:

The method of weighted residuals (MWR) is one of the approximation techniques for solving differential equations in FEM. One of these methods that will be presented in this thesis is Galerkin method:

The method of weighted residuals includes several approximation methods, and Galerkin method is one of them. This method was first introduced in 1915 and has been developed throughout the years to be one of the applicated methods in FEM (Finlayson & Scriven, 1966).

This method is based on reducing the number of errors in an assumed-mode method through turning the error into orthogonal error to a weighted function (Braun et al., 2002).

3.2 The decided approach for FEM in analyzing the hybrid floor-system with ANSYS APDL

In this part of the chapter of methodology, there will be presented the choices made in ANSYS APDL for the numerical investigation of the composite floor system. During the modelling in ANSYS, there have been experimented many approaches, however only the approaches that have given acceptable results will be presented.

3.2.1 Element types

The first approach in modelling was to try to make the problem as simple as possible. The aim was to reduce the time and the complexity of the modelling-process by choosing to model the experimental structure with a two-dimensional model (2-D). However, the results given by the 2-D model lacked the needed accuracy. Therefor it was decided to model the composite floor system in 3-D.

As was mentioned in the Introduction chapter, the composite floor consists of glulam beams (GL24h), OSB boards and a concrete layer with a 70 mm-thickness. It was chosen to use Structural SOLID for all three materials. For concrete, the library of ANSYS has a specific type of element which is SOLID65 (ANSYS, Inc,2011).

❖ **Glulam beams (GL24h)**

For the glulam beams it was decided to use structural SOLID type of element. SOLID185 and SOLID186 were of the used element types for modelling the glulam beams. As the following figures shows, SOLID186 has twenty nodes while SOLID185 has 8 nodes. Due to the high number of nodes in SOLID186, which made the model exceeds the allowed number of nodes in the ANSYS student version, it was chosen to model the beams with SOLID185.

Figure 15 The geometry of SOLID185 (8 nodes).
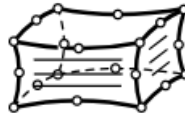
Figure 16 The geometry of SOLID186 (20 nodes).

SOLID185:

SOLID185 is used for three-dimensional modelling of solid structures. This type of element is defined by 8 nodes, each one of which has three degrees of freedom in the X-, Y- and the Z-direction, as shown in Figure 17. This element has the capabilities of plasticity, stress, large strain, and large deflection. It is also defined by the orthotropic material properties. (ANSYS, Inc, 2009), which has made it a perfect choice for modelling the glulam beams as they are of the orthotropic nature.
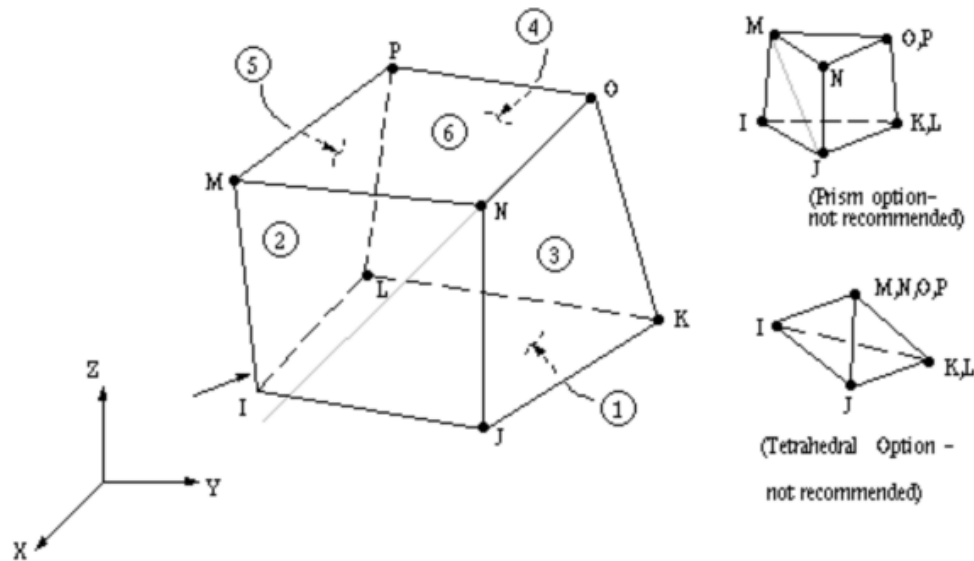
Figure 17 The geometry of SOLID185 with the nodes and the degree of freedom of these nodes. (ANSYS, Inc, 2011).

❖ **Oriented strand board (OSB)**

As OSB is of the same nature of glulam beams (orthotropic), it was decided to use SOLID185 as an element type for the modelling.

❖ **Concrete**

The finite element methods provide tools that simulate the reinforced concrete member and predict its response. ANSYS is one of FEM-software that provides a three-dimensional element specifically for concrete. An eight-nodes isoperimetric solid element that has integration points for both cracking and crushing tests. It provides a linear elastic behavior that governs the analysis until it exceeds the values of either the tensile or the compressive strength. The cracking or the crushing of concrete can be formed once the principal stresses reach compressive or tensile strength. This element is called SOLID65 (Dahmani et al., 2010).

SOLID65

A structural solid element with eight nodes that each has three degrees of freedom in X-, Y- and Z-direction. SOLID65 has the capabilities of plastic deformation, crushing and cracking in

three orthogonal directions. The following Figure 18 illustrates the locations of these nodes and the geometry of the element (ANSYS, Inc, 2011).
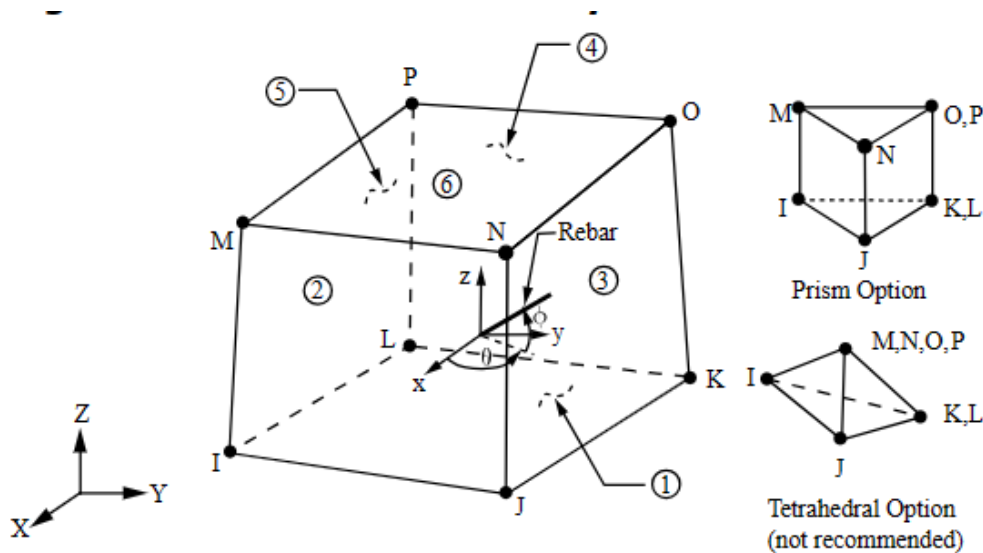
Figure 18 The geometry of SOLID65 with the nodes and degree of freedom (ANSYS, Inc, 2011).

3.2.2 Material Properties

In this section the properties of the materials used in FEM will be presented alongside the way some of these properties were calculated.

❖ **Glulam**

Some of the mechanical properties of glulam beams (GL24h) were provided in the experiment, such as the modulus of elasticity E_x = 11600 MPa. This value has been used in the calculation of other properties. It has been assumed that the glulam beams were made of Douglas-fir, and the elastic-ratio values in Forest Products Laboratory Wood Handbook were used. These values are presented in the following Table 7. Douglas-fir is among the only three species (Douglas-fir, Spruce-Sitka & Spruce-Engelmann) which have the values of (μ_{RL} & μ_{TL}) provided in the Handbook of Forest Product Laboratory. In addition, Douglas-fir gave values for modulus of elasticity, close to the values of EN 14080:2013 regarding GL24h. Therefore, Douglas-fir was chosen for this work.

Table 7 The values of elastic-ratio for some species of softwood. (Forest Product Laboratory, 2010).

Species	E_T/E_L	E_R/E_L	G_{LR}/E_L	G_{LT}/E_L	G_{RT}/E_L
Baldcypress	0.039	0.084	0.063	0.054	0.007
Cedar, northern white	0.081	0.183	0.210	0.187	0.015
Cedar, western red	0.055	0.081	0.087	0.086	0.005
Douglas-fir	0.050	0.068	0.064	0.078	0.007
Fir, subalpine	0.039	0.102	0.070	0.058	0.006
Hemlock, western	0.031	0.058	0.038	0.032	0.003
Larch, western	0.065	0.079	0.063	0.069	0.007
Pine					
Loblolly	0.078	0.113	0.082	0.081	0.013
Lodgepole	0.068	0.102	0.049	0.046	0.005
Longleaf	0.055	0.102	0.071	0.060	0.012
Pond	0.041	0.071	0.050	0.045	0.009
Ponderosa	0.083	0.122	0.138	0.115	0.017
Red	0.044	0.088	0.096	0.081	0.011
Slash	0.045	0.074	0.055	0.053	0.010
Sugar	0.087	0.131	0.124	0.113	0.019
Western white	0.038	0.078	0.052	0.048	0.005
Redwood	0.089	0.087	0.066	0.077	0.011
Spruce, Sitka	0.043	0.078	0.064	0.061	0.003
Spruce, Engelmann	0.059	0.128	0.124	0.120	0.010

By considering:

$$E_T/E_L \ = \ 0.050 \ \rightarrow$$

$$E_T \ = \ 0.050 \text{ x } 11600 = 580 \text{ MPa}$$

While

$$E_R/E_L \ = \ 0.068 \quad \rightarrow \qquad E_R \approx 789 \ MP$$

According to table 2 in section 2.1.3 the shear modulus of Gl24h is equal to 650 MPa. Nevertheless, it has been calculated using the elastic ratio in the previous table.

The following Table 8 shows the mechanical properties of GL24h used in ANSYS.

Table 8 The mechanical properties of glulam beams (GL24h) used as an input-data in ANSYS APDL.

Parameter	unit	value	source
E_X	MPa	11600	(Ferrara et al., 2023)
E_Y	MPa	580	Calculated using elastic ratio from Forest Products Laboratory.
E_Z	MPa	789	Calculated using elastic ratio from Forest Products Laboratory.
μ_{XY}		0.292	Forest Products Laboratory. Value for Douglas-fir
μ_{YZ}		0.390	Forest Products Laboratory. Value for Douglas-fir
μ_{XZ}		0.449	Forest Products Laboratory. Value for Douglas-fir
G_{XY}	MPa	742.4	Calculated using elastic ratio from Forest Products Laboratory.
G_{YZ}	MPa	81.2	Calculated using elastic ratio from Forest Products Laboratory.
G_{XZ}	MPa	904.8	Calculated using elastic ratio from Forest Products Laboratory.
Density	Kg/m^3	420	(Blab & Sandhaas, 2017)

❖ **Oriented strand board (OSB)**

Regarding the OSB it was assumed that the boards used in the experiment were of the class OSB/3, making them load-bearing boards for humid conditions, according to the classification of NS-EN300(SINTEF Building Research Design Guides, 2021). Another assumption for the thickness of the boards had to be made, giving OSBs the thickness of 22mm. As was mentioned in section (2.1.9) the modulus of elasticity for OSB is equal to 4930 MPa and the density is equal to 550 kg/m^3 (NS-EN12369-1). The given modulus of elasticity was used in the calculation of the other mechanical properties using the equation (5) in the section (2.1.10). The following Table 9 shows the mechanical properties for OSB that have been used as an input-data in ANSYS APDL.

Table 9 The values of the mechanical properties of the oriented strand boards (OSB) applied in the ANSYS model as input-data.

Parameter	Unit	Value	source
E_X	MPa	4930	NS-EN12369-1 (SINTEF, 2011)
E_Y	MPa	1980	NS-EN12369-1 (SINTEF, 2011)
E_Z	MPa	1980	NS-EN12369-1 (SINTEF, 2011)
μ_{XY}		0.202	(Plenzler et al., 2017)
μ_{YZ}		0.226	(Plenzler et al., 2017)
μ_{XZ}		0.239	(Plenzler et al., 2017)
G_{XY}	MPa	725.8	Calculated with Equation (5)
G_{YZ}	MPa	710.61	Calculated with Equation (5)
G_{XZ}	MPa	645.66	Calculated with Equation (5)
Density	Kg/m^3	550	NS-EN12369-1 (SINTEF, 2011)

❖ **Concrete**

The concrete slab in the timber-concrete composite floor system (TCC) consists of concrete of the C40/50 strength-class. The experiment provided two produced batches of concrete, where the two were tested according to EN12390-1. The cylindrical compression strength f_{CK}, the strain corresponding to maximum compression stress ε_{CU}, and the Young's modulus E_{CM} were provided as the mechanical properties for the two samples of concrete.

In this numerical investigation the sample with the higher mechanical properties' values was chosen. The following Table 10 shows the mechanical properties used in this numerical investigation, using ANSYS APDL.

Table 10 The mechanical properties of concrete from the physical experiment, used as input-data inside ANSYS APDL.

Parameter	Unit	Value	source
f_{CK}	MPa	43.5	(Ferrara et al., 2023)
ε_{CU}	%	0.43	(Ferrara et al., 2023)
E_{CM}	MPa	34200	(Ferrara et al., 2023)
μ		0.2	EN1992-1-1 §3.1.3(4)
Density	Kg/m^3	2500	EN 1992-1-1§3.1

3.2.3 Geometry

The published papers on the experiment conducted on the timber-concrete composite floor system (TCC) provided the geometry of the structure. TCC has an 8 meter-span with a width of 2.4 meters. However, the total thickness of TCC was not mentioned. The height of glulam beams and the thickness of the concrete slab were provided. To calculate the total thickness of TCC, the thickness of OSB had to be assumed to be 22 mm.

$$Total\ thicknes = \ the\ height\ of\ Gl24h\ + \ thickness\ of\ OSB$$
$$+ \ thickness\ of\ the\ concrete\ slab$$

The total thickness of TCC is 332 mm.

Figure 19, below, shows the geometry of the beam-frame provided by the physical experiment (Ferrara et al., 2023).
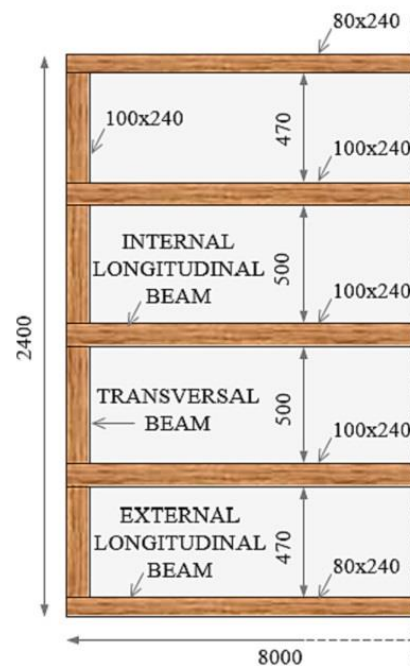
Figure 19 Plan from below of the timber-concrete composite floor shows the beam-frame with the geometry. (Ferrara et al., 2023).

The timber-concrete composite (TCC) floor system has the required symmetry to model a part of the structure. However, the numerical results showed a significant variation from the physical experimental results. Therefore, it was decided to model the whole TCC system. Figure 20 is taken from the model in ANSYS and shows the Gl24h beam-frame.
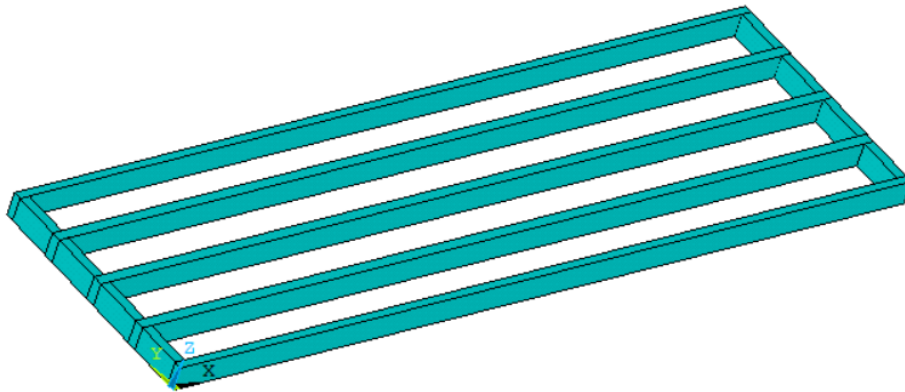
Figure 20 The geometry of the glulam beams-frame inside the FEM-simulation in ANSYS APDL.

The following Figure 21 was taken from the FEM-simulation in ANSYS, where it shows the total geometry of the TCC floor system (Glulam beams-frame, OSB & concrete slab).
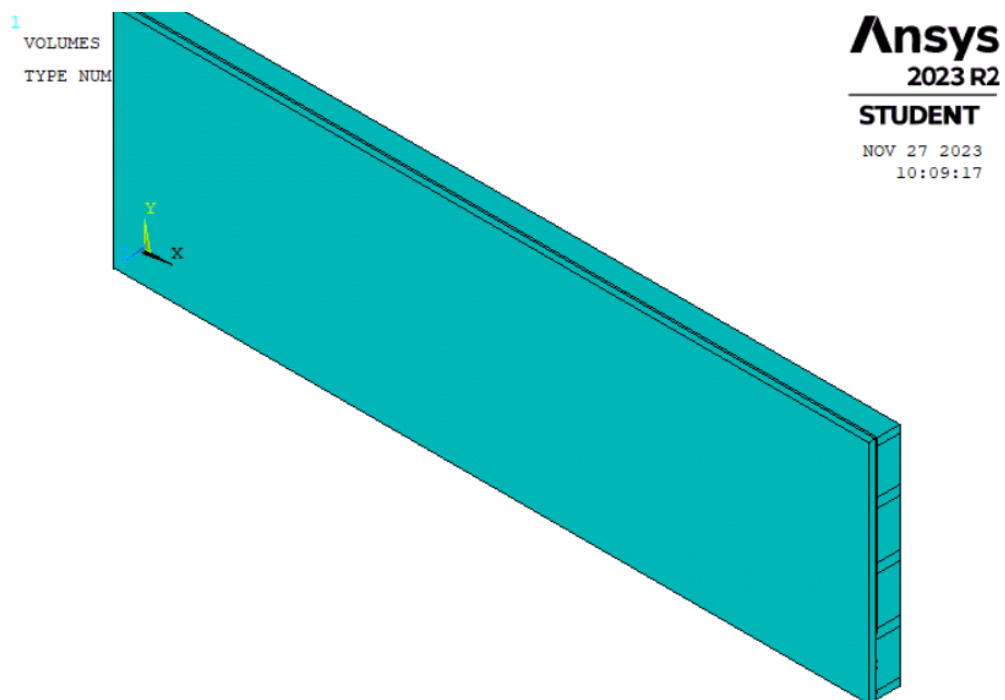
Figure 21 The modelled geometry of the timber-concrete composed floor system in ANSYS APDL.

3.2.4 APDL commands

VGLUE:

VGLUE is a command in ANSYS APDL that generates new volumes by gluing volumes. The glued volumes must share areas along their common boundaries. VGLUE results in the merging of keypoints, lines, and areas at the common volume boundaries.

Menu path:

Main Menu>Preprocessor>Modeling>Operate>Booleans>Glue>Volumes.

VGLUE command was used in this FEA to glue the glulam beams together and glue the beams-frame with the OSB. Figure 22 taken from the model in APDL ANSYS shows the lines of the volumes, where it is noticed that the lines at the shared areas had been generated in distinct colors. That means that the volumes are successfully glued together.

Figure 22 The plotted lines of the geometry for the beam-frame and the OSB, where they illustrate that the volumes are glued together.

3.2.5 Meshing

Meshing is considered as one of the most crucial steps in executing an accurate simulation using finite element analysis (FEA). A meshed element will consist of nodes that represent the shape of the geometry. There are two types of meshing methods that will be presented as the following:

- **Tetrahedral** element meshing (tet): For complex geometries.

- **Hexahedral** element meshing (hex): hex or brick elements have more accurate results than tet for lower elements count.

However, there exist several additional meshing methods that have more locally controlled meshes, such as sweep meshing.

Sweep meshing: This method allows for sweeping the mesh through the volume and faces resulting in an efficient mesh that has regular sizing through the whole volume.

The quality of the mesh is crucial for more precise results. However, it may result in more invested time for meshing and solving the FEA.

For this numerical investigation, it was decided to use a hexahedral meshing method and sweep it through the volumes. The source elements for the meshing are quadrilateral.

In addition, it was chosen to pick the sectional lines of the volumes and decided a "number of element divisions" of at least 3. (3 for the OSB boards, 7 for the concrete slab). This allowed for a respectable quality of mesh, inside the limitation of the student license.

3.2.6 Constraints

The timber-concrete composite floor system (TCC) was described in the experiment as linearly supported at two edges (Ferrara et al., 2023). Figure 23 shows the floor system supported linearly with two beams. The four-point loading test was executed by a hydraulic jack with loading apparatus. The hydraulic jack was attached to a portal frame that was fully restrained to the floor. The two linear supports in the figure are considered as horizonal rollers where the TCC can move horizontally (X-direction) and is restrained vertically. The portal frame prevented TCC from moving horizontally in both X- and Z-direction.

In the FEA model the portal frame was replaced with a pin support at one of the two linear beams. Figure 23 illustrates the constraints used to prevent TCC from moving horizontally, in both X- and Y-direction.

Figure 23 The four-point bending test applied on the TCC floor system in the physical experiment (Ferrara et al., 2023).

Inside the ANSYS's model only the nodes along the lower corners were restrained as Figure 24, shows.

Figure 24 The constraints in the lower edges of the TCC floor system inside the ANSYS model. Nodes in the left edge retrained in Z-direction while in the right edge in both Z and X.

In addition, TCC had to be restrained to prevent the movement in the Y-direction. Therefore, it was decided to restrain the outer areas of the two external longitudinal beams. Figure 25 taken from APDL model shows the two restrained areas.
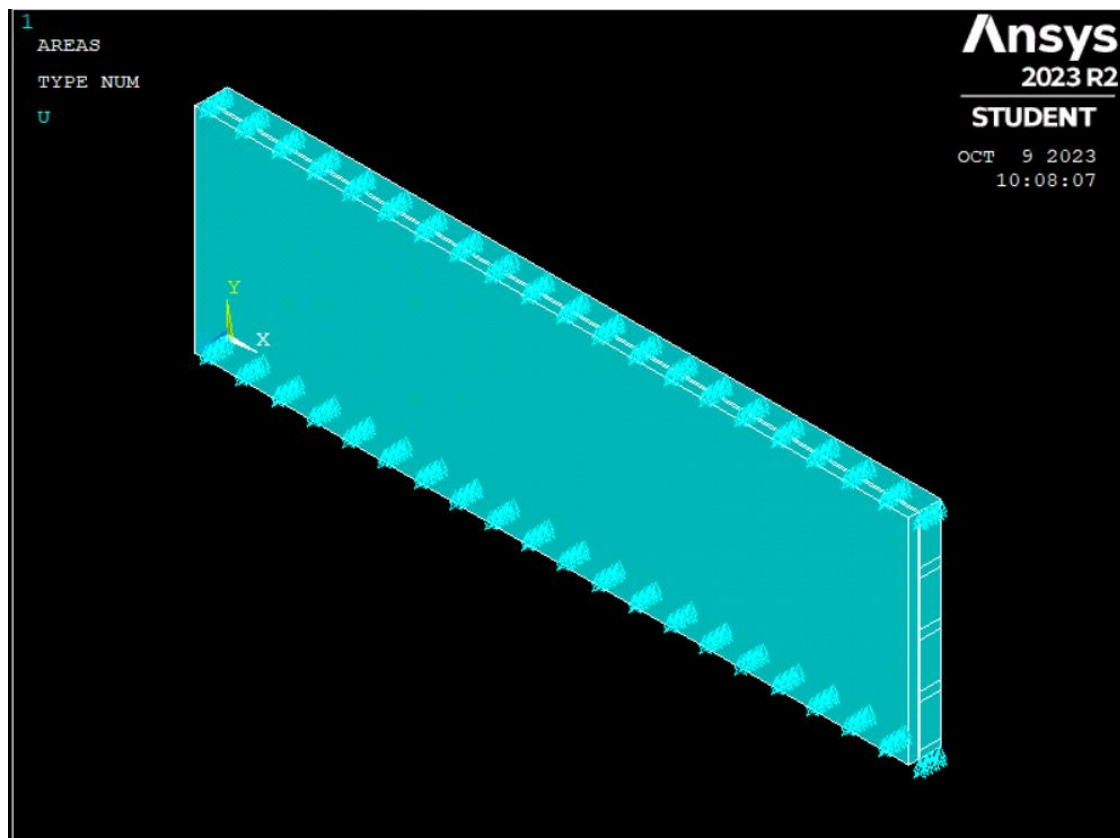
Figure 25 Illustrates the two restrained outer areas of the two external longitudinal beams inside the model in ANSYS.

3.2.7 Contact element

A contact element is an element used to define the behavior between parts of the model that are touching each other's. There are several types and shapes of contact elements In ANSYS mechanical APDL. These types will be summed up in the following points (ANSYS, Inc, 2011):

- Surface-to-surface.
- Line-to-surface.
- Node-to-surface.
- Line-to-line.
- Node-to-node contact element.

The contact element is considered a complex phenomenon that adds nonlinearities to the finite element simulation. Furthermore, the level of complexity raises when the finite element model is simulating a composite system (Hybrid). In this case the contact element is considered as a hybrid connection, where it must interact between varied materials. For the simulation of three-dimensional structural solid finite elements, the contact interfaces with surface-to-surface contact elements (Tsalkatidis et al., 2018).

The type of contact applicated for this work is a contact element that connects two three-dimensional structural solids. These volumes are the OSB and the concrete slab. Therefore, a surface-to-surface type of contact element was used.

To define a contact between parts of a model a target and a contact must be selected. ANSYS recommends that the more rigid should be selected as a target while the less rigid as a contact. In addition, the target surface can be either defined as a TARGE or CONTRA, where TARGE is for only rigid surfaces while CONTRA for deformable surfaces (ANSYS, Inc., 2004). For this simulation, the following elements were chosen:

CONTA174

CONTA174 has the same geometric characteristics as the structural solid element chosen for both the OSB and the concrete slab (SOLID185). This element is a three-dimensional with 8 nodes and high-order quadrilateral on the surface of 3-D solid element (ANSYS, Inc., 2004). The following Figure 26, shows the geometry of CONTA174 (ANSYS, Inc, 2010).
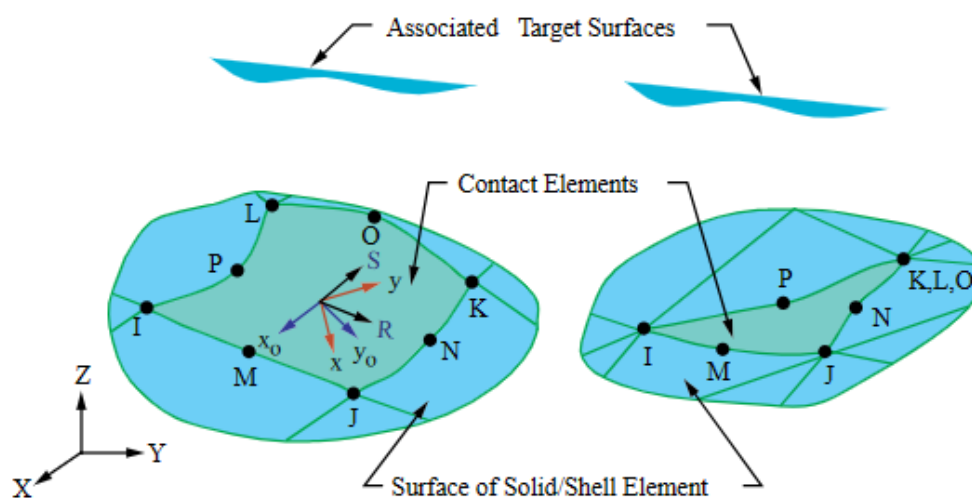
Figure 26 The geometry of contact element CONTA174 (ANSYS, Inc, 2010).

TARGE170

TARGE170 is an element that is used to represent a 3-D target associated with the contact element CONTA174. The geometry of TARGE170 is shown in Figure 27 where, as described, it is associated with surface-to-surface contact element.
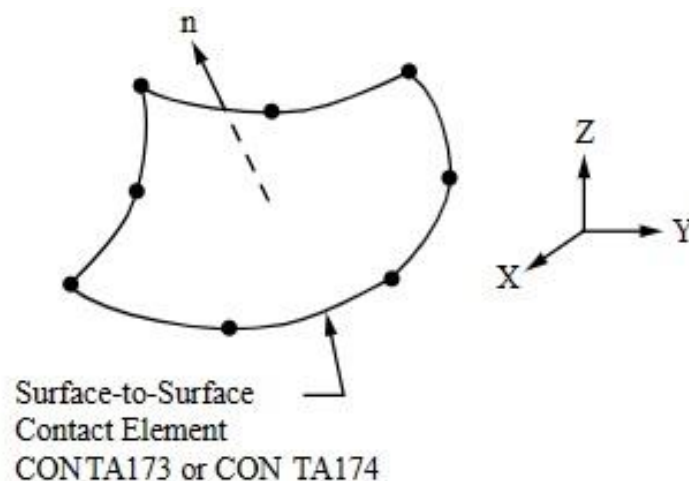
Figure 27 The geometry of the element TARGE170. (ANSYS, Inc, 2010).

When the contact and the target are selected, the coefficient of the friction of the contact element is to be defined. In the case of this work, the connection is between OSB (orthotropic) and the concrete slab (isotropic). The contact element for timber-concrete composite systems (TCC) is assumed to be frictional. The value of the frictional coefficient for TCC, according to some experiments, varies from 0.3 to 0.68. However, it is suggested that the lowest values are conservative choices for design purposes (Jaaranen & Fink, 2020). Therefore, a value of 0.3 for the frictional coefficient, was assumed for this finite element simulation.

One of the most crucial properties of a contact element is the normal penalty stiffness factor (FKN), which has a default value of 1. However, ANSYS contact technology guide suggests using a smaller value if bending deformation dominates. The suggested value is FKN = 0.1. In addition, it is suggested that determining a respectable stiffness value requires some experimentation. One of the suggested procedures is to use a low value for the contact stiffness as a start, as it is better to underestimate the value rather than overestimating it. Usually, the penetration problems resulted by using a low stiffness are less challenging to solve than the convergence's difficulties caused by high stiffness assumptions (ANSYS, Inc,

2004). Therefore, the normal penalty stiffness for this simulation was experimented starting from the lowest (0.1). However, the one that gave a deformation result close to the experiment was 0.2. The contact element is shown in Figure 28.
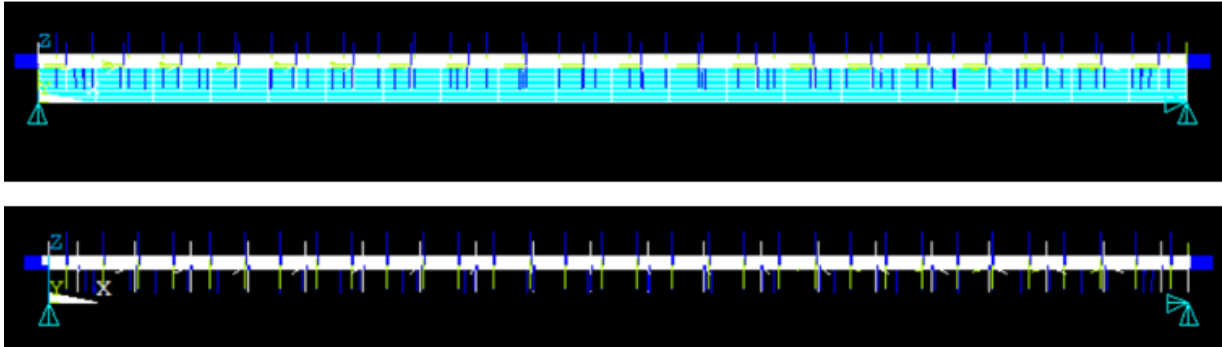
Figure 28 illustrates the contact element between OSB and the concrete slab inside the model in ANSYS APDL

3.2.8 Loads

The timber-concrete composite (TCC) floor system was subjected to a four-point bending test. For the finite element simulation. The applicated forces with the resulted displacement in the physical experiment are presented in the following Table 11.

For this work, it was decided to apply the structural loads (S_5 = 247.9 KN) on the nodes in the negative z-direction. The load was divided into the number of nodes constructing a line on the surface of the concrete slab. Two lines of nodes with two meters distanced from each other's.

Table 11 The maximum forces applicated on timber-concrete composite floor system with the maximum resulted displacement (Ferrara et al., 2023).

Specimen	F_{max} [kN]	$d_{o,max}$ [mm]
S_1	228.6	55.8
S_2	241.7	68.5
S_3	245.8	62.7
S_4	261.4	73.1
S_5	247.9	63.6
av.	245.1	64.7
coef. var	4.8 %	10.0 %

Figure 29 below, taken from the FEM-simulation, illustrates the force applied on the nodes. The forces are presented with the red arrows shown in the middle of the timber-concrete composite floor system.

Figure 29 shows the applied loads as forces on nodes in the negative z-direction. The red arrows illustrate the forces.

3.3 Parametric studies

A parametric study is an analysis conducted to investigate the influence of different physical or geometric parameters on both the problem and the result. It depends on making assumptions on the different parameters and evaluating the sensitivity of the analysis to these parameters. For this work it was decided to do three parametric studies and four finite element simulations in ANSYS APDL. These parametric tests will be presented as following:

3.3.1 Parametric study-1 The concrete slab

This analysis was conducted of the timber-concrete composite floor system by assuming new geometries for the concrete slab. Two different simulations, where it was assumed two different thicknesses of the concrete slab. The two simulations will be presented in the following points:

- **Simulation 1**: reducing the thickness of the concrete slab by 20 mm (from 70 mm to 50 mm).
- **Simulation 2**: increasing the thickness of the concrete slab by 20 mm (from 70 mm to 90 mm)

3.3.2 Parametric study-2 The glulam beams

The glulam beams in the experiment were of the strength-class GL24h. For this analysis it was assumed GL30h as a new strength-class for the glulam beams, while the geometries of the beams remain the same. The following Table 12, shows the changes made to the mechanical properties inside the model in ANSYS.

Table 12 The values of the mechanical properties for glulam beams (GL30h) used as input-data in ANSYS model, for Parametric study 2.

Parameter	unit	value	source
E_X	MPa	13600	(Blab & Sandhaas, 2017)
E_Y	MPa	680	Calculated using elastic ratio from Forest Products Laboratory.
E_Z	MPa	925	Calculated using elastic ratio from Forest Products Laboratory.
μ_{XY}		0.292	Forest Products Laboratory. Value for Douglas-fir
μ_{YZ}		0.390	Forest Products Laboratory. Value for Douglas-fir
μ_{XZ}		0.449	Forest Products Laboratory. Value for Douglas-fir
G_{XY}	MPa	870.4	Calculated using elastic ratio from Forest Products Laboratory.
G_{YZ}	MPa	95.2	Calculated using elastic ratio from Forest Products Laboratory.
G_{XZ}	MPa	1060.8	Calculated using elastic ratio from Forest Products Laboratory.
Density	Kg/m^3	480	(Blab & Sandhaas, 2017)

3.3.3 Parametric study-3 The placement of the load

This analysis is conducted on the timber-concrete composite (TCC) floor system by changing the placement of the four-point loading test. The loads in the experiment were applied on TCC in the middle part, with a two meters distance between the two steel beams that transferred the loads to the concrete slab. The distance between the steel beams that are transferring the loads has increased to four meters. Figure 29, in section (3.2.8) shows the original placement of the loads, while Figure 30 & Figure 31 illustrate the new placement of the loads.

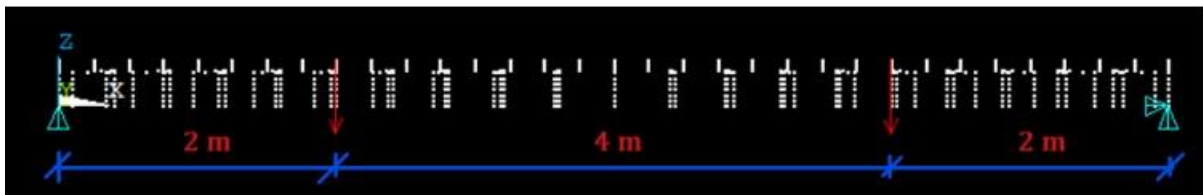*Figure 30 (X, Z) plan view of the new placement of the applied loads inside the model of ANSYS for Parametric study (3).*

The red arrows represent the loads applied as structural forces on the nodes, pointing in the negative z-direction, simulating the four-point bending test applied on the timber-concrete composite floor system.
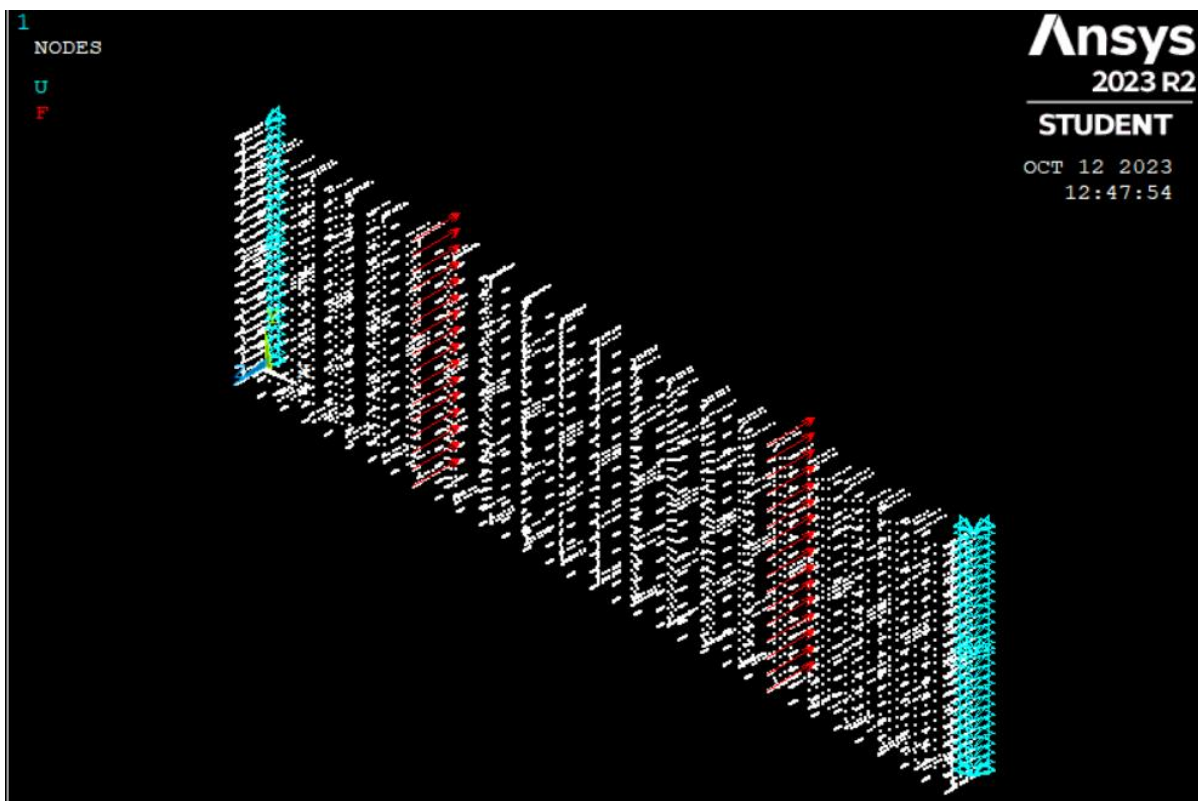
Figure 31 3D plan view of the applied loads for Parametric study (3).

4 Results

During this work, there were conducted five finite element analyses with ANSYS APDL R2 2023. In this chapter, there will be presented results of the five FEM-simulations. These results will be presented in the form of figures taken from these different simulations. The results will include the following:

1. The maximum displacement in the timber-concrete composite floor system.
2. Von Mises stresses (tensile, compressive and shear).
3. Stresses in contact elements between OSB and concrete slab (Total stress).

4.1 FEM-Simulation of the physical experiment

The simulation of the physical experiment aims to get the same displacement, resulting in the physical experiment in a computational simulation using ANSYS APDL. The results of this simulation are as following:

4.1.1 Displacement

The following Figure 32 shows the resulted displacement in the timber-concrete composite floor system after the application of the four-points bending test, applying a load equal to 247.9 KN. The maximum displacement is equal to 63.61 mm resulted in the mid-span of the timber-concrete composite floor system.
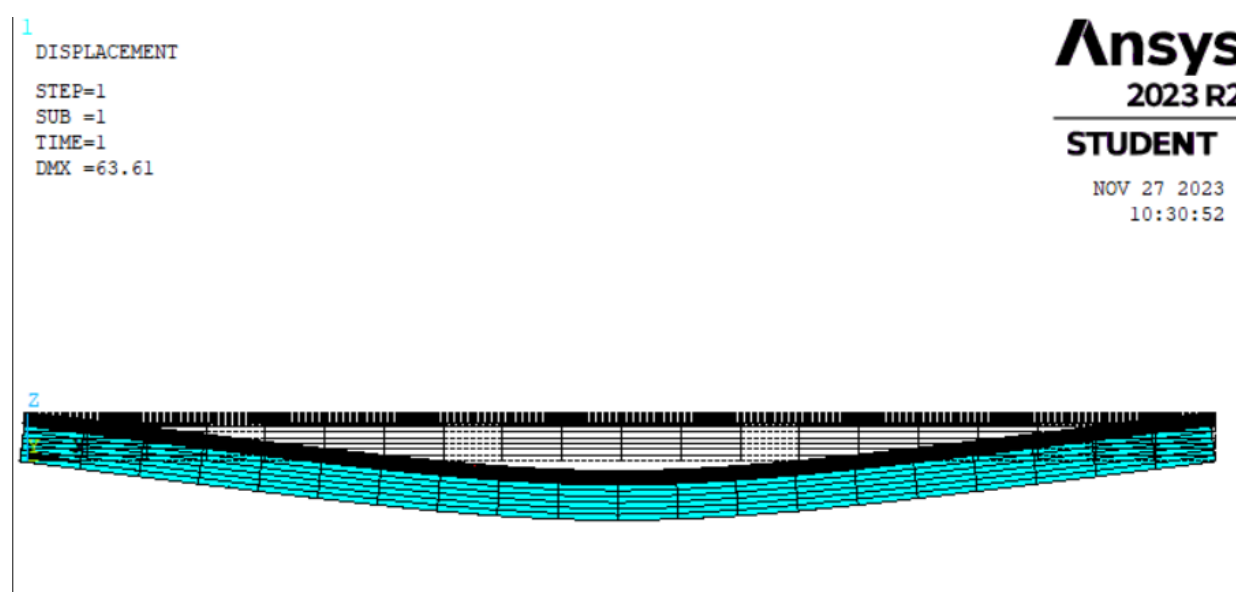
Figure 32 The maximum displacement in the TCC floor system resulted by a 247.9KN four-point bending test.

4.1.2 Von Mises stresses

The following Figure 33, presents the von Mises stresses distribution in the timber-concrete composite floor system resulted by the application of the four-points bending test (247.9 KN).

A value of 30.64 N/mm^2 for a load of 247.9 KN.
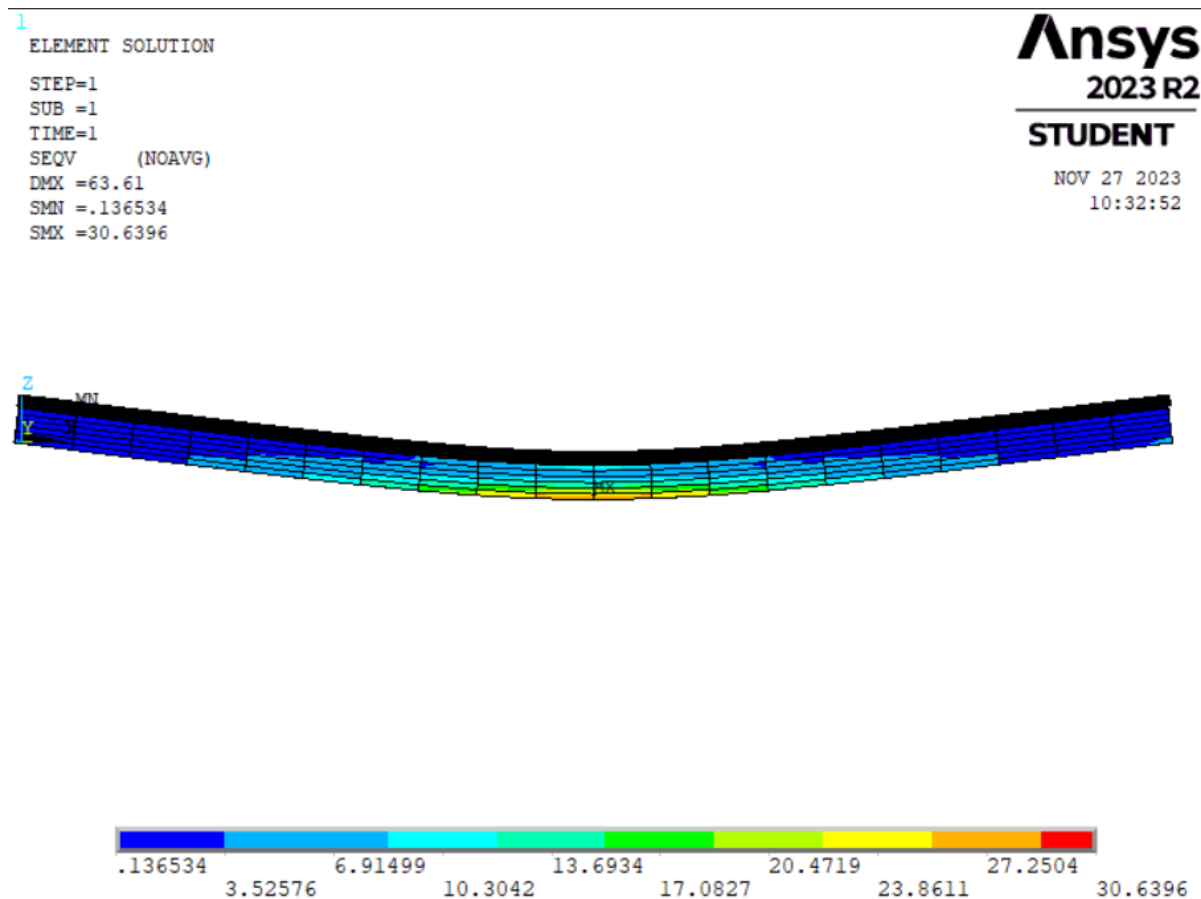
Figure 33 Von Mises stresses in the TCC floor system in response to 249.7 KN; 4-point bending test.

The stresses are most critical in the lower parts of the glulam beams in the mid-span of the TCC floor system. Figure 34 shows the highest values of von Mises stress in the middle 3 beams of the beam-frame.

The red color represents the value of ≥ 27.25.

Orange ≥ 23.86

Yellow ≥ 20.47

Light green ≥ 17.08

Green ≥ 13.69
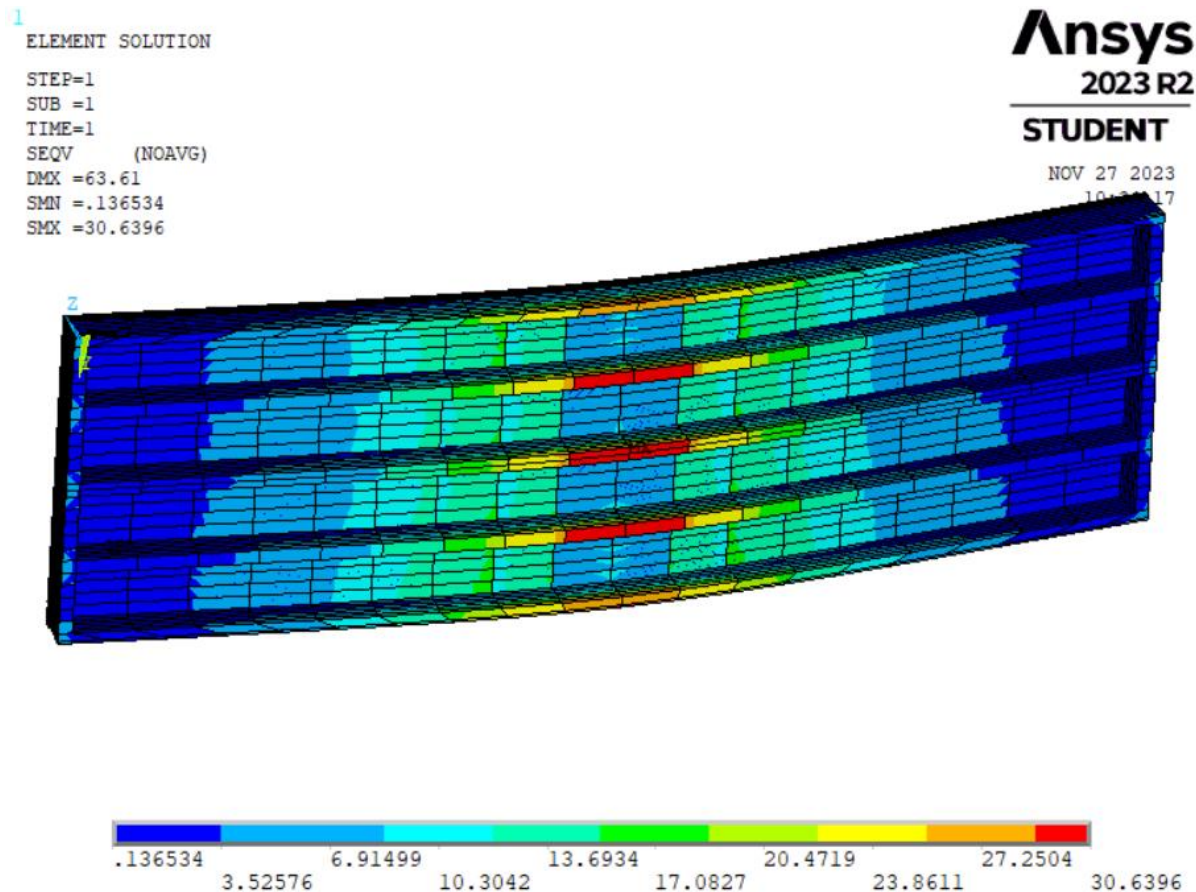
Figure 34 3D-view of the TCC floor system showing the von Mises stresses at the bottom.

4.1.3 Total stresses in the contact element

Total stresses in the contact elements have the maximum value of 0.366 N/mm². Figure 35 shows that the stresses in the contact elements exist under the applied load (247.9 KN) and have the maximum values at the edges of the timber-concrete composite floor system. The most critical values are greater than 0.326 N/mm², presented by the red color.
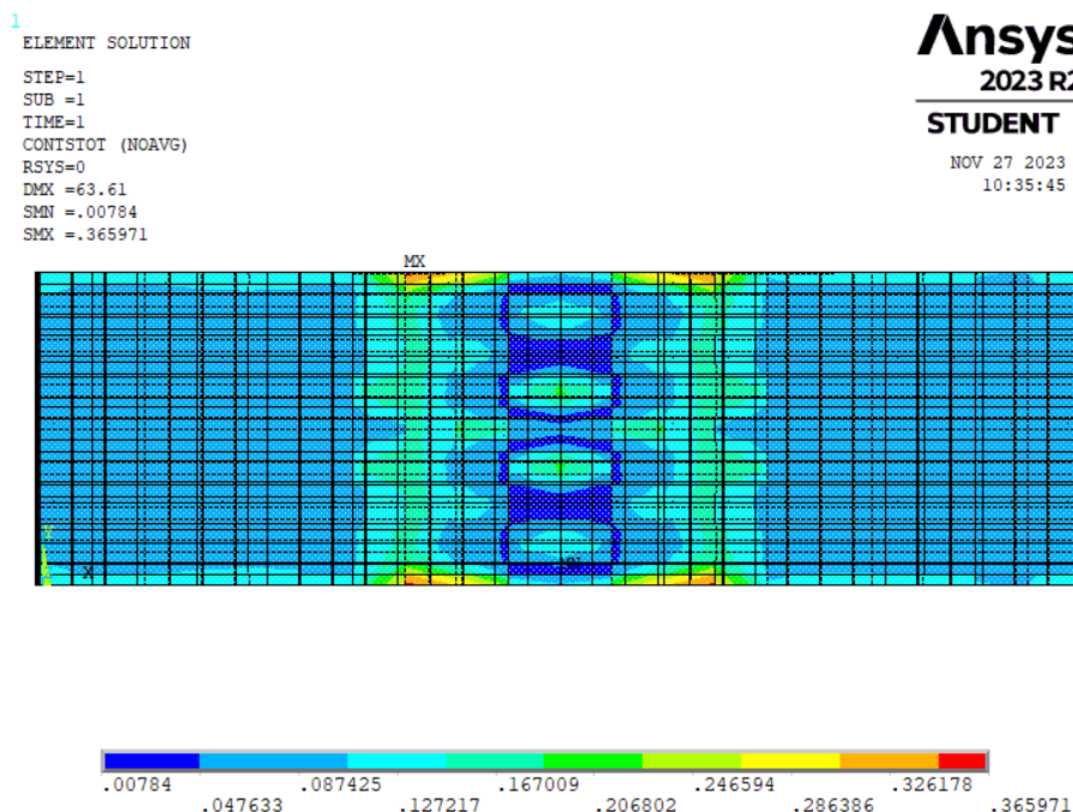
Figure 35 (X,Y)-plan view of the contact elements, showing total stresses.

4.2 FEM-simulations of Parametric study 1

The first parametric analysis is the investigation of the effect of the concrete slab's thickness. This analysis consists of two FEM-simulations where the thickness of the slab was reduced by 20 mm in the first, while increased by 20 mm in the second. The results of these two simulations will be presented as following:

4.2.1 Maximum displacement of TCC floor with 50 mm thick concrete slab

The maximum displacement in the timber-concrete composite floor system increased by approximately 10 mm, as a result for reducing the thickness of the concrete slab from 70 mm to 50 mm. The new value of the maximum displacement is equal to 73.35 mm as shown in Figure 36.

1
DISPLACEMENT

STEP=1
SUB =1
TIME=1
DMX =73.3468

Ansys
2023 R2
STUDENT
NOV 27 2023
10:38:34

Figure 36 Maximum displacement of the TCC floor system for parametric study-1 with 50mm-thick concrete slab.

4.2.2 Von Mises stresses of TCC floor with 50 mm thick concrete slab

Von mises stress in the timber-concrete composite floor system increased from 30.64 to 34.71 N/mm^2, because of reducing the thickness of the concrete slab from 70 mm to 50 mm. The most critical values of the stresses are in the bottom of the glulam beams at mid-span. The following Figure 37 shows the highest values in the 3 middle longitudinal beams. The red color represents von Mises stresses with values $\geq$ 30.86 N/mm^2.
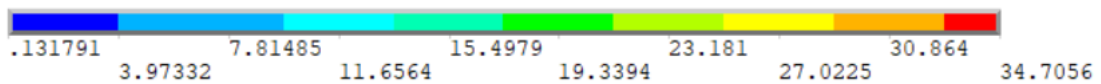
Figure 37 Back view of the TCC floor system (bottom) shows von mises stresses.

4.2.3 Total stresses in contact elements with 50 mm thick concrete slab

The total stresses in the contact elements between the OSBs and the concrete slab increased from 0.366 N/mm2 to 0.413 N/mm2, as a result of reducing the thickness of the concrete slab by 20mm. The most critical values of stresses remained to be at the edges of the TCC floor system. The stress values $\geq$ 0.367 are presented in the red color as shown in Figure 38.
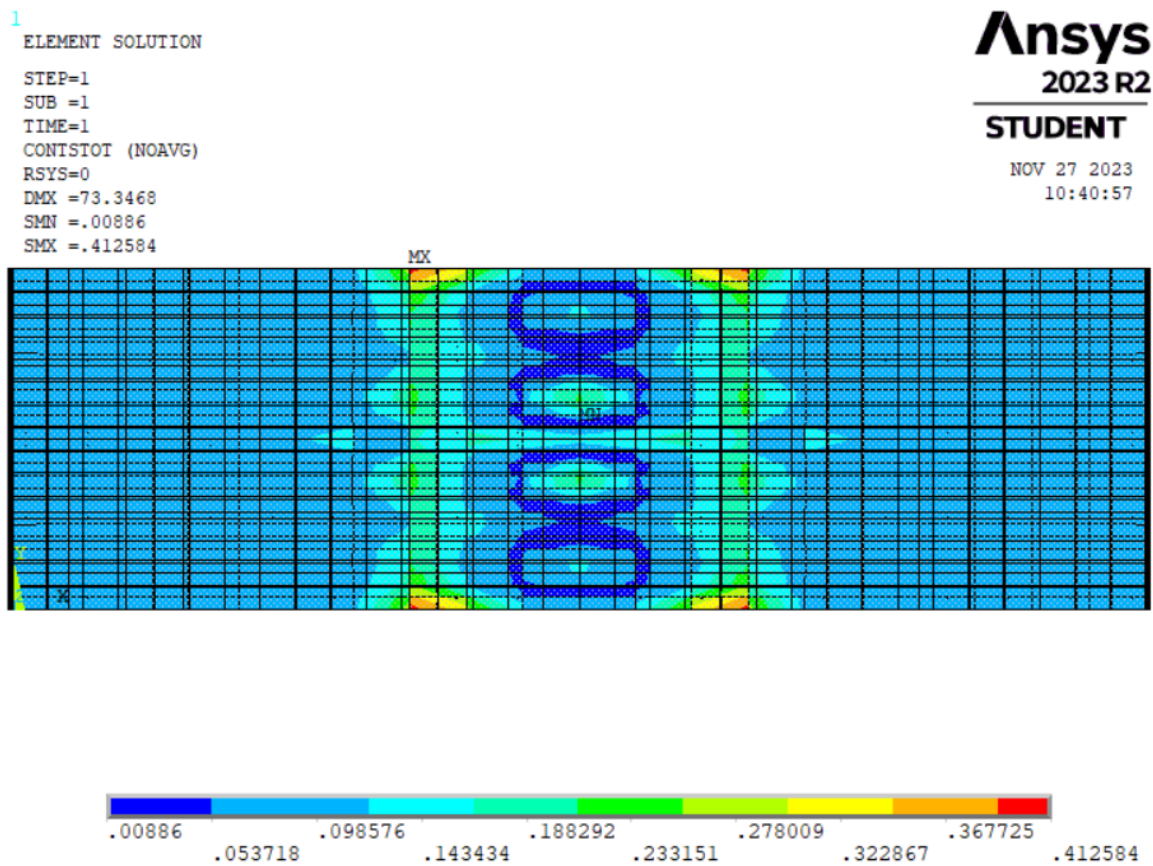
Figure 38 Total stresses in contact elements for parametric study -1 for 50 mm thick concrete slab.

4.2.4 Maximum displacement for TCC floor with 90 mm thick concrete slab

The maximum displacement of the TCC floor system was reduced by approximately 6 mm by increasing the thickness of the concrete slab from 70 mm to 90 mm. The following Table 13 shows the comparison in the maximum displacement between the numerical analysis of the physical experiment (70 mm concrete), the first simulation of parametric study-1 and the second simulation of parametric study-1. The maximum displacement in TCC floor system with the increased concrete thickness is presented in Figure 39.

Table 13 The maximum displacement in the computational simulation of the physical experiment, the 1st, and 2nd simulations of parametric study 1.

FEM-simulation	Thickness of concrete slab	Maximum displacement	Figure
Physical experiment FEM-simulation	70 mm	63.61 mm	32
Parametric study 1, 1st simulation	50 mm	73.35 mm	36
Parametric study 1, 2nd simulation	90 mm	57.12 mm	39
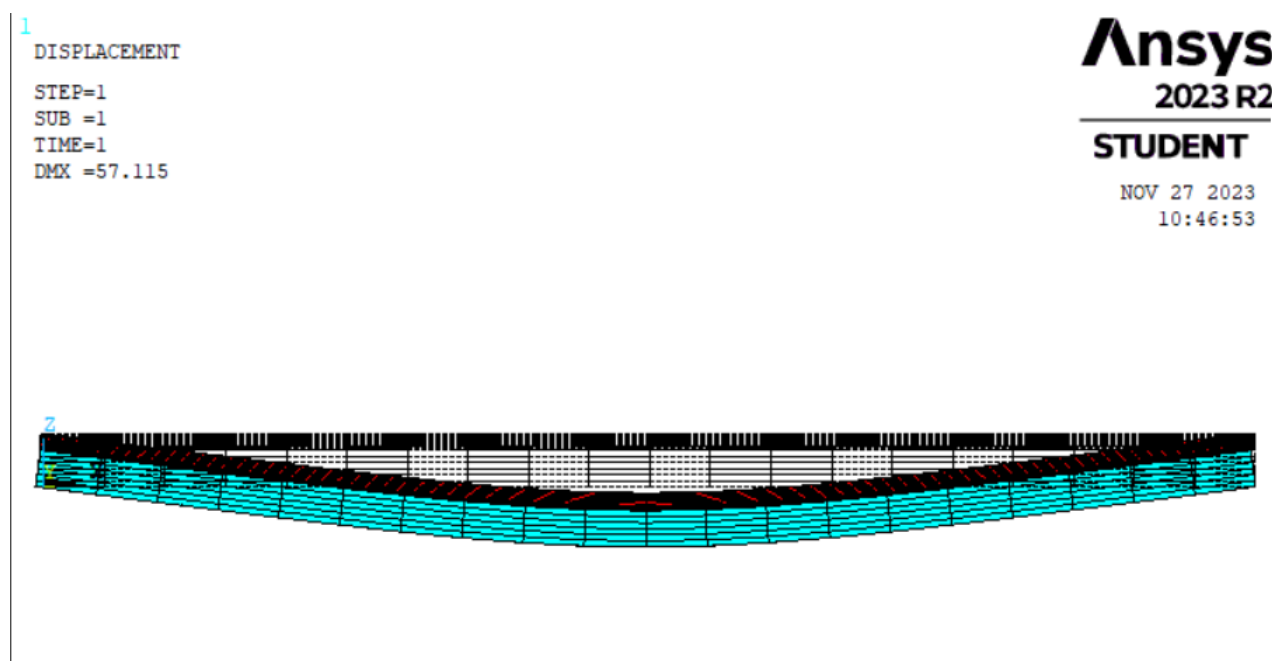
Figure 39 Maximum displacement in the TCC floor system for parametric study-1 for 90 mm thick concrete slab

4.2.5 Von mises stress for TCC floor with 90 mm thick concrete slab

The von Mises stresses in TCC floor system decreased by 4 N/mm^2 because of increasing the thickness of the concrete slab. The comparison between the values of von Mises stresses for the 1st ,2nd and 3rd FEM-simulations are presented in the following Table 14.

Table 14 Von Mises stresses for the simulations of the physical experiment, the 1st, and the 2nd simulations of parametric study 1.

FEM-simulation	Thickness of concrete slab	Von Mises stresses	Figure
Physical experiment's simulation	70 mm	30.64 N/mm^2	33 & 34
Parametric study 1, 1st simulation	50 mm	34.71 N/mm^2	37
Parametric study 1, 2nd simulation	90 mm	26.43 N/mm^2	40
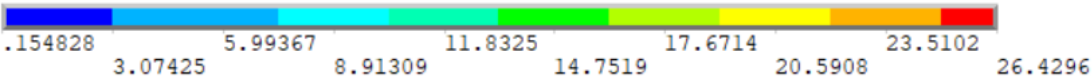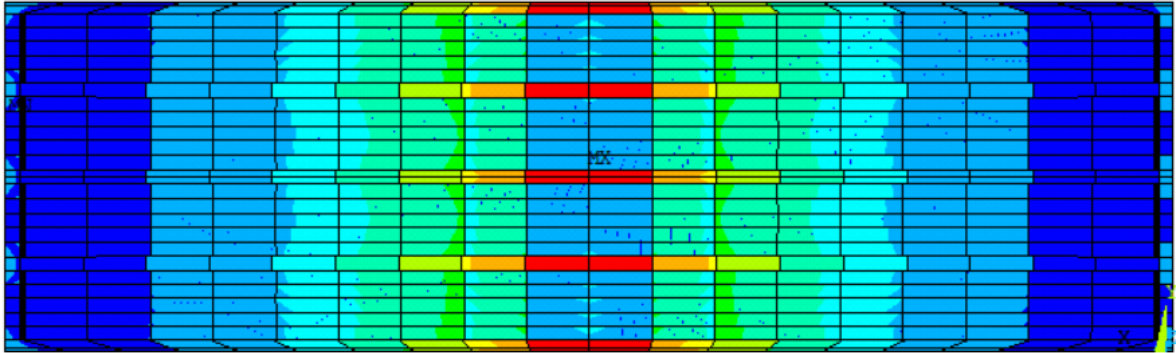
Figure 40 Von Mises stresses in the TCC floor system for Parametric study-1 for 90 mm concrete slab.

4.2.6 Total stresses in contact elements for 90 mm concrete slab

The following Figure 41, shows the total stresses in the contact elements between OSB and the 90mm-concrete slab. The maximum value of stresses in the contact element is equal to 0.326 N/mm^2. The comparisons between the total stresses in the contact elements for the first three FEM-simulations are presented in Table 15.

Table 15 The total stresses in the contact element for the physical experiment's simulation, the 1st, and the 2nd simulations of parametric study 1.

FEM-simulation	Thickness of concrete slab	Total stress in contact element	Figure
Physical experiment FEM-simulation	70 mm	0.366 N/mm^2	35
Parametric study 1, 1st simulation	50 mm	0.413 N/mm^2	38
Parametric study 1, 2nd simulation	90 mm	0.326 N/mm^2	41
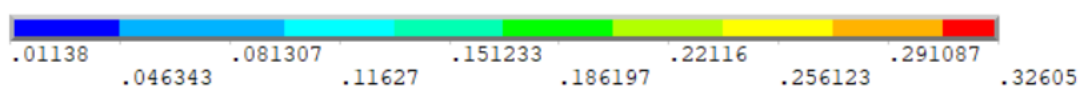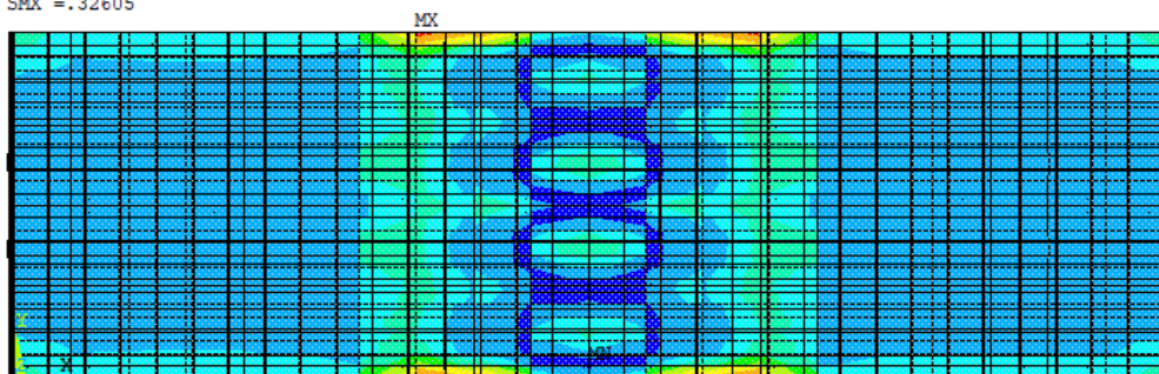
Figure 41 Total stresses in contact elements between the OSB and the 90mm-concrete-slab.

4.3 FEM-simulation for Parametric study 2

This parametric analysis is conducted on the timber-concrete composite floor system, by changing the strength classification of the glulam beam from GL24h to GL30h. The aim is to investigate the effect of the mechanical properties of glulam beams on the numerical results. The results of the FEM-simulation will be presented as the following:

4.3.1 Maximum displacement

The maximum displacement in the TCC floor system was decreased from 63.45 mm to 60.61 mm after changing the strength classification of the glued laminated timber beams to GL30h. The maximum displacement is shown in Figure 42.

DISPLACEMENT

STEP=1
SUB =1
TIME=1
DMX =60.6135

Ansys
2023 R2
STUDENT

NOV 27 2023
10:54:37

Figure 42 The maximum displacement in the TCC floor system for Parametric study 2; (GL30h).

4.3.2 Von Mises stresses

Von Mises stresses in the timber-concrete composite floor system has increased from 30.64 N/mm^2 to 31.92 N/mm^2 as shown in figure 43. The figure shows the bottom of the TCC floor system. The red color represents the most critical value of von Mises stresses. The bottoms of the beams at mid-span are the most parts subjected to critical stresses.
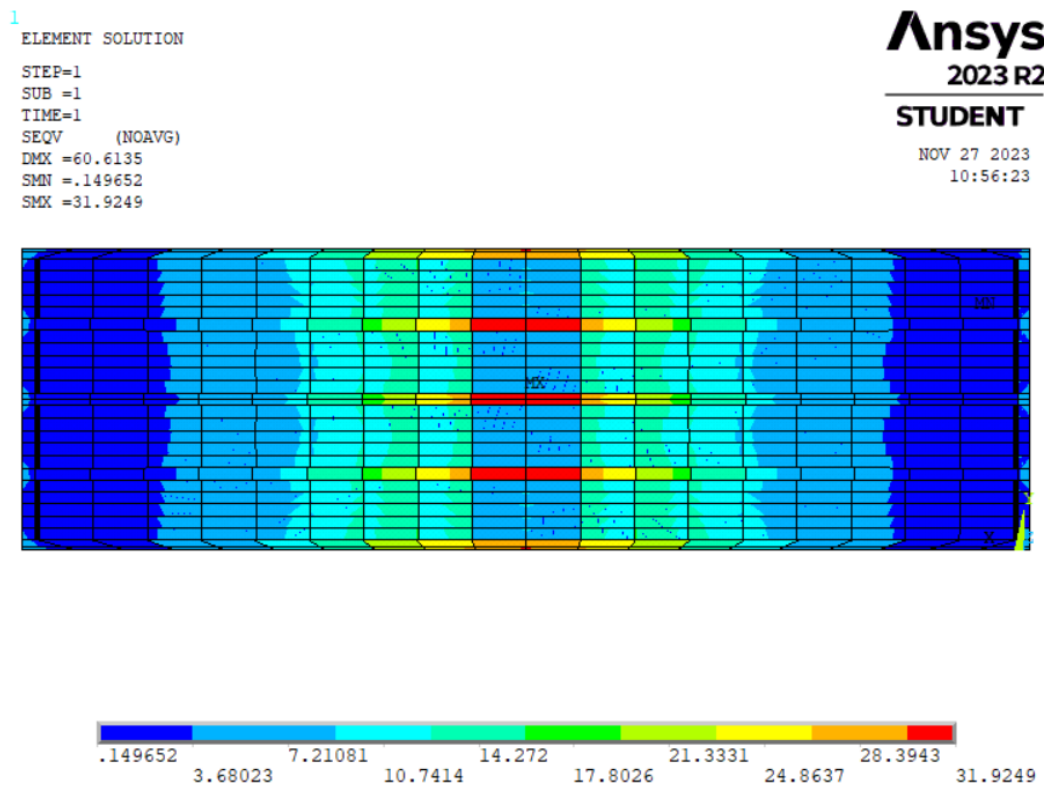
Figure 43 The back view of the TCC floor system shows von Mises stresses in the bottom of the glulam beams.

4.3.3 Total stresses in contact elements

The total stresses in the contact elements for Parametric study 2 are presented in Figure 44. The maximum value of the stresses has decreased from 0.366 N/mm^2 for the FEM-simulation of the physical experiment to 0.355 N/mm^2 for the new strength class of glulam beams (GL30h). The most critical values of the stresses are around the edges of the TCC floor system.

```
1
ELEMENT SOLUTION
STEP=1
SUB =1
TIME=1
CONTSTOT (NOAVG)
RSYS=0
DMX =60.6135
SMN =.008174
SMX =.355204
                                    MX
```

Ansys
2023 R2
STUDENT
NOV 27 2023
10:57:20

```
.008174        .085291        .162409        .239527        .316645
    .046733        .12385        .200968        .278086        .355204
```
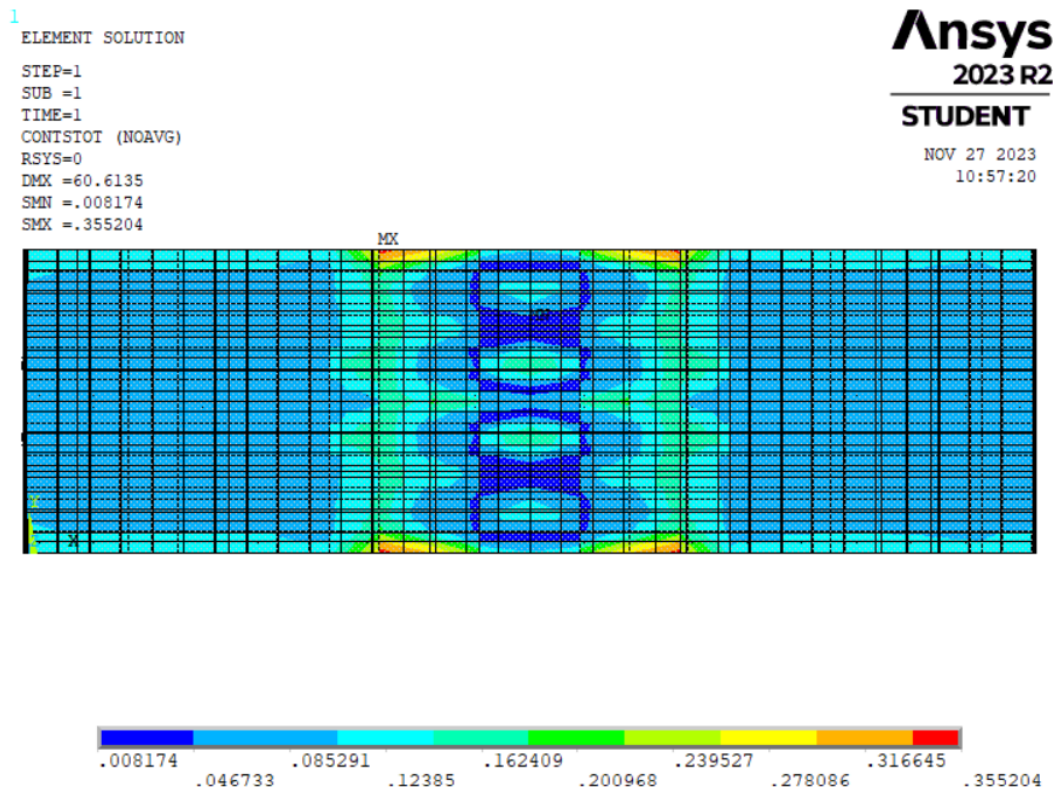
Figure 44 Total stresses in the contact element for Parametric study 2; (GL30h).

4.4 FEM-simulation for Parametric study 3

This analysis is conducted on the timber-concrete composite floor system by changing the placement of the four-points bending test, applying the loads closer to the supports. The results of the FEM-simulation will be presented as the following:

4.4.1 Maximum displacement

The maximum displacement in the timber-concrete composite floor system was reduced from 63.45 mm to 45.29 mm. Reduction of approximately 18 mm for same load (247.9 KN) by moving the loads towards the supports of the TCC floor system. The maximum displacement is presented in Figure 45.
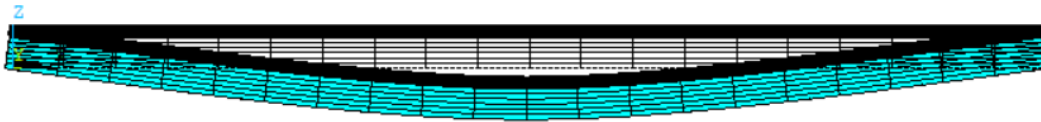
Figure 45 (X,Z)-plan view of the TCC floor system, showing the maximum displacement for parametric study 3, (New load placement).

4.4.2 Von Mises stresses

The stresses in the TCC floor system were reduced from 30.64 N/mm^2 to 20.45 N/mm^2 as Figure 46 shows. Moving the loads towards the supports of the TCC floor system reduced the concentrated stress in the mid-span. The most critical values of von Mises stresses remained to be at the bottom of the middle three longitudinal glulam beams.

ELEMENT SOLUTION
STEP=1
SUB =1
TIME=1
SEQV   (NOAVG)
DMX =45.2943
SMN =.132262
SMX =20.4548

.132262   4.64837   9.16448   13.6806   18.1967
   2.39032   6.90643   11.4225   15.9387   20.4548
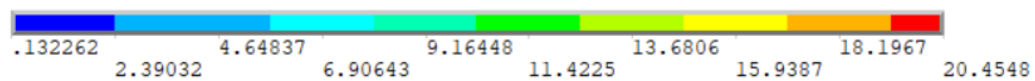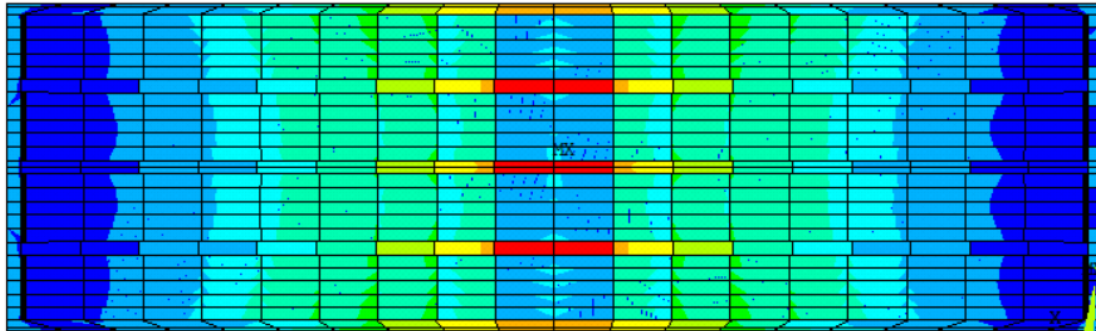
Figure 46 (X, Y)-plan view from the bottom shows von Mises stresses in the TCC floor system.

4.4.3 Total stresses in contact elements

The total stresses in the contact elements between the oriented strand boards (OSB) and the concrete slab were decreased from 0.366 N/mm² to 0.245 N/mm². Less stress in the contact element caused by the new placement of the four-point bending test as Figure 47 shows.

```
1
ELEMENT SOLUTION

STEP=1
SUB =1
TIME=1
CONTSTOT (NOAVG)
RSYS=0
DMX =45.2943
SMN =.005341
SMX =.24494
                    MX
```

```
.005341        .058586        .11183        .165074        .218318
      .031964        .085208        .138452        .191696        .24494
```
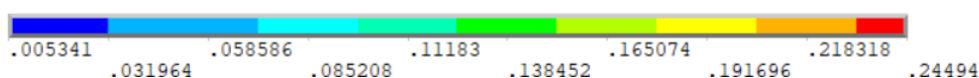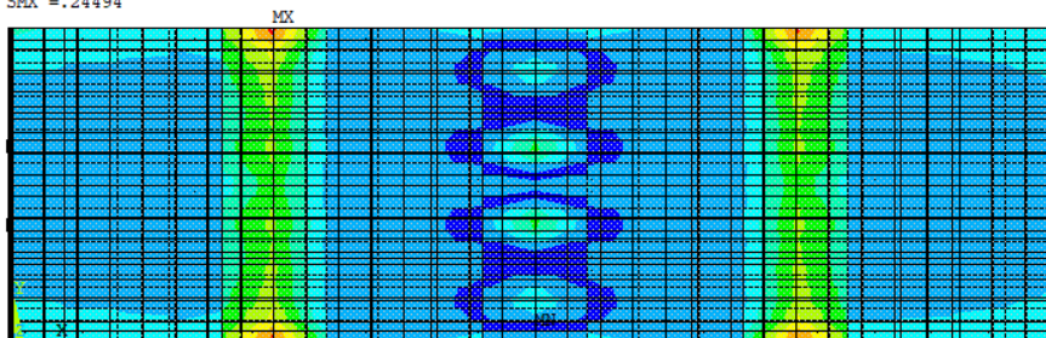
Figure 47 (X, Y)-plan view of the TCC floor system showing total stresses in contact elements.

Summary of the numerical results of the five numerical analyses is presented in Table 16.

Table 16 The numerical results of the five FEM-simulations.

FEM-Simulation	Maximum displacement (mm)	Von Mises stresses (N/mm²)	Total stresses in contact elements (N/mm²)	comment
FEM-Simulation of the physical experiment	63.61	30.64	0.366	Physical experiment (Ferrara et al., 2023).
Parametric Study 1	73.35	34.71	0.413	50 mm thick concrete slab.
	57.12	26.43	0.326	90 mm thick concrete slab.
Parametric study 2	60.61	31.92	0.355	New strength class for glulam beams (GL30h).
Parametric study 3	45.29	20.45	0.245	New placement for the loads.

5 Discussion

In this chapter of the thesis, the results from chapter 4 will be discussed, considering the verification of the FEM-simulation of the physical experiments and the results of the parametric studies. This part will be presented as the following:

5.1 The verification of the 3D-modell

The aim of creating a three-dimensional computational model with FEM-modeling-software is to accurately simulate the timber-concrete composite floor system used in the physical experiment. An accurate result of the numerical model, which matches the result of the physical experiment, would allow for further investigation, in the form of parametric studies. Therefore, creating an accurate FEM-simulation of the physical experiment is the most crucial part of this numerical investigation. The parametric studies allow for a deeper analysis of the influences of the different parameters composing the investigated floor system.

The deviation of the numerical results from the experimental results is preferred to be small. However, the result of the FEM-simulation of the physical experiment, has a deviation of less than 0.0002 %. The maximum displacement of the timber-concrete composite floor system, resulted by 247.9 KN four-point bending test is equal to 63.6 mm, as shown in Tabel 11 in chapter 4. Correspondingly, the maximum displacement of the timber-concrete composite floor system resulted in the numerical analysis conducted with ANSYS is equal to 63.61 mm, as presented in Figure 32 in chapter 4.

There have been several factors that contributed to the achievement of such a satisfactory numerical result, such as the properties of the contact elements between the OSB and the concrete slab. As was mentioned in the methodology chapter, the contact element has a crucial influence on the results of the numerical analysis. The contact element is necessary to connect two materials of different natures. The oriented strand boards (OSB), as presented in the theory chapter, have an orthotropic nature, while the concrete is an isotropic material. Therefore, the properties of the contact element have been magnificently influential on the sensitivity of the numerical results. The properties of the contact element in ANSYS APDL have default values that usually work for the different mechanical analysis.

However, for this numerical analysis of a composite structure, it was required to change the default values of some of the properties in order to achieve accurate results. These properties will be presented as the following:

- *"The normal penalty stiffness of the contact element (FKN)"* The default value of the FKN factor is equal to one. Nevertheless, ANSYS contact technology guide suggested to underestimate the value of FKN, rather than overestimating it. The normal penalty stiffness of the value 0.2 was suitable for this numerical analysis, as it gave an accurate maximum displacement that matched the result of the physical experiment.

- "The behavior of contact element surface" The default behavior of the surface of the contact element caused failure in the numerical analysis, as the OSB separated itself from the concrete slab. The rigidity of the timber-concrete composite floor system was in doubt. By contrast, changing the behavior to "bonded always" assured the rigidity of the timber-concrete composite floor system, and made it deflect like a one unit without separations.

In addition, there were several choices that have had an influence on the numerical results, such as the "element types." As was mentioned in the methodology chapter, the aim was to make the problem as simple as possible. The first approach was to model the timber-concrete composite floor system with a two-dimensional model, due to the less time and effort required. The element types used for the two-dimensional model were "BEAM161" for the modelling of the beams and "SHELL181" for OSB and concrete combined. This approach gave results that did not match the results of the physical experiment. Therefore, it was decided to model the timber-concrete composite floor system with a three-dimensional model, choosing SOLID185 for glulam beams and OSB and SOLID65 for concrete.

5.2 Parametric studies

The parametric studies are based on changing some of the physical and geometrical parameters of the timber-concrete composite floor system to investigate the influence of these different parameters on the flexural behavior of timber-concrete composite floor system. The results of the four FEM-simulations presented in chapter 4 will be discussed in this part of the discussion chapter.

5.2.1 Parametric study 1

The first parametric study was conducted on the timber-concrete composite floor system to investigate the influence of thickness of concrete slab on the numerical results. This study has two FEM-simulations where the thickness of the concrete slab was reduced by 20 mm in the first, while increased by 20 mm in the second.

- Reducing the thickness of the concrete slab from 70 mm to 50 mm has resulted in increasing of the maximum displacement, Von Mises stresses and the total stresses in the contact element. The result of the maximum displacement increased by approximately 13 %. From 63.6 mm to 73.35 mm, as shown in Figure 36, Table 13 & Table 16.

  Von Mises stresses in the TCC floor system increased by around 12 %, Figures 33 & 34 show Von Mises stresses in the TCC floor system subjected to the physical experiment, where it is noticeable that the most affected part is the bottom of the glulam beams. These stresses are caused by the tension in the bottom of the TCC floor system. The reduction of the thickness of the concrete slab caused an increased Von Mises stress from 30.64 N/mm^2 to 34.71 N/mm^2, as presented in Figure 37.
  Furthermore, the total stresses in the contact element increased by 11%, as explained in Table 15. The total stresses in the contact element in the physical experiment's 3D-model is equal to 0.366 N/mm^2, as shown in Figure 35, while Figure 38 presents the total stress in contact element after reducing the thickness of the concrete slab.

- Increasing the thickness of the concrete slab from 70 mm to 90 mm has resulted in reducing the maximum displacement, Von Mises stresses, and total stresses in contact element. The result of the maximum displacement decreased from 63.61 mm to 57.12, as shown in Figure 39. An approximate reduction of 10 % in the maximum displacement.

  Furthermore, von Mises stresses in the TCC floor system fallen from 30.64 to 26.43 N/mm^2, as presented in Figure 40. The stresses in the TCC floor system decreased by almost 14 %.

  Similarly, the total stress in the contact element between OSB and the concrete slab was reduced by circa 11 %. The value of total stresses in the contact element, after increasing the thickness of the concrete slab, is equal to 0.326 N/mm^2 (Figure 41).

Although von Mises stresses in the timber-concrete composite floor system decreased due to the increased thickness of the concrete slab, the result of the numerical analysis showed that the stresses in the external longitudinal glulam beams reached critical values. The two external longitudinal glulam beams had a smaller cross-sectional area (80 x 240) than the three middle longitudinal beams (100 x 240). The increase of the stresses in the external beams is due to the increase of the self-wight of the TCC floor system, which caused an increase in the tension at the bottom of the beams. The critical values of the stresses are presented in the red color in Figure 41.

5.2.2 Parametric study 2

The second parametric study is based on changing the mechanical properties of the glued laminated timber beams. The aim is to investigate the effect of the strength class of glulam beams on the numerical results and the flexural behavior of TCC floor system. The strength classification of glulam beams used in the physical experiment was of the class GL24h (Ferrara et al., 2023), while, in this numerical analysis, the strength class was increased to GL30h.

The results of the numerical investigation showed a slight reduction in the maximum displacement of the timber-concrete composite floor system. A maximum displacement of 60.61 mm opposed to 63.61 mm (5 % reduction), as shown in Figure 42.

Although the maximum displacement of TCC floor system decreased, due to the higher strength-class of glulam beams, von Mises stresses increased in the results of the numerical analysis. The value of von Mises stresses rose from 30.64 N/mm^2 to 31.92 N/mm^2 as

presented in Figure 43. However, total stresses in the contact elements reduced from 0.366 to 0.355 N/mm2 as shown in Figure 44.

The changes in results, due to the change of the strength classification of glulam beams, have not been crucially significant. However, the reduction in the maximum displacement is the only noticeable result of this numerical analysis.

5.2.3 Parametric study 3

This parametric analysis is based on changing the placement of the loads in the four-point bending test applied on the timber-concrete composite floor system. The TCC floor systems spans 8 meters, where the four-point bending test is applied on the middle 2 meters, as shown in Figure 1. The four-point bending test in this parametric analysis was applied on the middle four meters, by moving the loads towards the supports, as shown in Figure 30. The aim is to investigate the effect of the placement of the loads on the numerical results of the flexural behavior of the timber-concrete composite floor system.

The numerical result of the maximum displacement was reduced by 29 %, due to the change of loads placement. The maximum displacement dropped from 63.61 mm to 45.29 mm, as shown in figure 45.

Similarly, von Mises stresses in the timber-concrete composite floor system was decreased by 33 %. Von mises stresses dropped from 30.64 N/mm^2 to 20.45 N/mm^2, as presented in Figure 46.

Furthermore, total stresses in the contact elements were reduced significantly. The numerical result presented in Figure 47 shows total stresses in the contact elements is equal to 0.245 N/mm^2. A 33 % reduction in total stresses in contact element has been monitored, due to the new placement of the loads. However, the stresses in the contact elements appeared to be more concentrated under the loads, as shown in Figure 47. The distance between the two lines of loads is increased, which made the four-point bending test applied on a larger area. Although it has reduced the total stresses in the contact elements, it made it more concentrated under these two lines of nodes; that the loads were applied on.

6 Conclusion

The aim of this thesis was to numerically simulate the flexural behavior of timber-concrete composite (TCC) floor system, which is linearly supported at two edges and subjected to a four-point bending test. The geometry of the TCC floor system is based on the geometry of the physical experiment of Ferrara et al., (2023). The model of the numerical analysis is verified against the results of the physical experiment. Simulating the TCC floor system was significantly challenging, due to the different materials and the complexity of timber. However, the three-dimensional model of the physical experiment gave a promising result, which matched the result of the physical experiment accurately. The accurate result of the numerical analysis made a strong base for another four models, in a form of parametric studies. The aim of the parametric studies was to investigate the effect of the different parameters of the TCC floor system (Concrete, Glulam beams, and load placement) on the results of the flexural behavior. A justification behind the successful modelling approach, with ANSYS APDL, of timber-concrete composite structures will be concluded with, in the following points:

- Three-dimensional modelling approach for both glulam beams and concrete.
- Using the command "select entities" for selecting (volumes, elements...etc.) consistently.
- Meshing the different materials separately, before connecting them together.
- Choosing fractional, surface-to-surface contact element for connecting the materials of different natures. (Timber and concrete for this work).
- Underestimating the value of the "normal penalty stiffness factor" (FKN), with an experimental approach; starting from the lowest value. Especially when bending deformation dominates.
- "The behavior of contact element surface" should be "Bonded always" for the timber-concrete composite structure to act like one unit.

On the other hand, the first two parametric analyses conducted on the timber-concrete composite floor system have shown that the concrete slab has the most significant effect on the behavior of the hybrid system. The thickness of the concrete slab has a crucial influence on both the displacements and the stresses in the TCC floor system. The larger the thickness of the concrete slab is, the lesser displacement and stresses occur in the timber-concrete composite floor system. The second parametric study showed that the increase of the strength classification of glulam beams was not as crucial as increasing the thickness of the

concrete slab. Therefore, it was concluded that the thickness of the concrete slab has a greater influence on the flexural behavior of the timber-concrete composite floor system.

Nevertheless, the placement of the loads influences both the displacement and the stresses significantly, especially for long-span TCC floor systems. Avoiding concentrated loads in the mid-span would reduce displacements and stresses. The numerical results of the third parametric study showed an approximate reduction of 30 % in both maximum displacement and stresses in the TCC floor system. The loads were moved towards the supports as presented in Figure 30.

Finally, this research has shown the potential of the accurate simulation of TCC composite floor systems with FEM-software, and hopefully will be an addition to further research.

7 Further Work

Even though the numerical analysis showed the promising potential of timber-concrete composite floor systems, there are still many unanswered questions. In this chapter there will be presented some of the open-questions that can be a base for further research in investigating the potentials of timber-concrete composite floor systems.

Some of these open questions will be presented in the following points:

➢ The long-term behavior of the components of timber-concrete composite floor systems.

➢ The effect of the types of the different mechanical connections between timber and concrete, on the flexural behavior.

➢ Post-failure behavior of the TCC floor systems.

➢ The influence of the length of the span on vibration and natural frequency of TCC floor systems.

➢ Analyzing the effect of thickness of concrete slab on vibrations and natural frequencies.

8 Bibliography

Ahmadi, M., & Kioumarsi, M. (2023). Predicting the elastic modulus of normal and high strength concretes using hybrid ANN-PSO. Materials Today: Proceedings.

ANSYS, Inc. (2004). Ansys contact technology guide. Release 9.0

ANSYS, Inc. (2009). Theory reference for the mechanical apdl and mechanical applications. Release 12.

ANSYS, Inc. (2011). Ansys mechanical apdl element reference. Release 14.0

APA (2017) Sustainable building, sustainable future. APA, Washington D.C

ARCWOOD- CLT and Glulam structures manufacturer. Glulam - Arcwood

Ashkenazi, E. K. (1978). Anizotropia drewesiny i drewesnykh materialow. Moskwa: Lesnaya Promyshlennost.

Asiri, A. M., & Mohammad, A. (Eds.). (2018). Applications of nanocomposite materials in dentistry. Woodhead Publishing.

ASTM, C. (2008). Standard test method for fundamental transverse, longitudinal, and torsional resonant frequencies of concrete specimens. Annual book of ASTM standards.,69+50

Australian Government, Forest and Wood Products Research and Development Corporation (FWPRDC)(2006) Forest, wood and Australia's carbon balance. Australian Government, Forest and Wood Products Research and Development Corporation, Australia

Bajaber, M. A., & Hakeem, I. Y. (2021). UHPC evolution, development, and utilization in construction: A review. Journal of Materials Research and Technology, 10, 1058-1074.

Bi, Z. (2017). Finite element analysis applications: a systematic and practical approach. Academic Press.

Blab, H. J., & Sandhaas, C. (2017). Timber engineering principles for design. KIT Scientific Publish-Ing. (B6) (pp.105-113)

Braun, S., Ewins, D. J., & Rao, S. S. (2002). Encyclopedia of vibration. (No Title).

Byggforsk, S. I. N. T. E. F. (2021). 571.050 OSB-boards. Types and properties.

Clough, R. W. (2004). Early history of the finite element method from the viewpoint of a pioneer. International journal for numerical methods in engineering, 60(1), 283-287.

Cook, R. D. (2007). Concepts and applications of finite element analysis. John wiley & sons.

Dahmani, L., Khennane, A., & Kaci, S. (2010). Crack identification in reinforced concrete beams using ANSYS software. Strength of materials, 42, 232-240.

Delatte, N. J. (2001). Lessons from Roman cement and concrete. Journal of professional issues in engineering education and practice, 127(3), 109-115.

Dong, L., Xu, H., Fan, P., & Wu, Z. (2021). On the Experimental Determination of Poisson's Ratio for Intact Rocks and Its Variation as Deformation Develops. Advances in Civil Engineering, 2021, 1-10.

Edition, C. (2010). Wood Handbook. Forest Products Laboratory - (5-1) - (5-3): (pp. 90-93)

Ellobody, E., Feng, R., & Young, B. (2013). Finite element analysis and design of metal structures. Elsevier.

European Standards (2013)- BS EN 14080:2013 Timber structures. Glued laminated timber and glued solid timber. Requirements (en-standard.eu)

Ferrara, G., Michel, L., & Ferrier, E. (2023). Flexural behaviour of timber-concrete composite floor systems linearly supported at two edges. Engineering Structures, 281, 115782.

Finlayson, B. A., & Scriven, L. E. (1966). The method of weighted residuals—a review. Appl. Mech. Rev, 19(9), 735-748.

Fischer, C. (2016). Density and bending properties of Norway spruce (Picea abies (L.) Karst.) structural timber–Inherent variability, site effects in machine strength grading and possibilities for presorting.

Gosselin, A., Blanchet, P., Lehoux, N., & Cimon, Y. (2017). Main motivations and barriers for using wood in multi-story and non-residential construction projects. BioResources, 12(1), 546-570.

Holschemacher, K., Klotz, S., & Weibe, D. (2002). Application of steel fiber reinforced concrete for timber-concrete composite constructions. Lacer, 7, 161-170.

Jaaranen, J., & Fink, G. (2020). Frictional behaviour of timber-concrete contact pairs. Construction and Building Materials, 243, 118273.

Khormani, M., & Jaari, V. R. K. (2023). Statistical analysis of the compressive strength of concrete using 2D DIP technology and Finite Element Method. Case Studies in Construction Materials, 19, e02461.

Kremer, P. D., & Symmons, M. A. (2015). Mass timber construction as an alternative to concrete and steel in the Australia building industry: a PESTEL evaluation of the potential. International Wood Products Journal, 6(3), 138-147.

Lamothe, S., Sorelli, L., Blanchet, P., & Galimard, P. (2021). Lightweight and slender timber-concrete composite floors made of CLT-HPC and CLT-UHPC with ductile notch connectors. Engineering Structures, 243, 112409.

Landis, E. N., & Bolander, J. E. (2009). Explicit representation of physical processes in concrete fracture. Journal of Physics D: Applied Physics, 42(21), 214002.

Lehringer, C., & Gabriel, J. (2014). Review of recent research activities on one-component PUR-adhesives for engineered wood products. Materials and joints in timber structures: recent developments of technology, 405-420.

Li, Z., Zhou, X., Ma, H., & Hou, D. (2022). Advanced concrete technology. John Wiley & Sons.

Melchiorre, M. & Duncan Th. (2021). The fundamentals of FEA meshing for structural analysis. ANSYS BLOG. ANSYS Inc.

Mirdad, M. A. H., Daneshvar, H., Joyce, T., & Chui, Y. H. (2021). Sustainability design considerations for timber-concrete composite floor systems. Advances in Civil Engineering, 2021, 1-11.

Natterer, J., Hamm, J., & Favre, P. (1996, October). Composite wood-concrete floors for multi-story buildings. In Proceedings of the international wood engineering conference (Vol. 3, pp. 431-435).

Nepomuceno, M. C., & Bernardo, L. F. (2019). Evaluation of self-compacting concrete strength with non-destructive tests for concrete structures. Applied Sciences, 9(23), 5109.

Ong, C. B. (2015). Glue-laminated timber (Glulam). Wood composites, 123-140.

Papadrakakis, M., & Sapountzakis, E. (2017). Matrix methods for advanced structural analysis. Butterworth-Heinemann.

Plenzler, R., Ludwiczak-Niewiadomska, L., & Strzelecki, P. (2017). Elastic and strength properties of OSB layers. Drvna industrija, 68(1), 3-9.

Plüss, Y., & Zwicky, D. (2014). A case study on the eco-balance of a timber-concrete composite structure in comparison to other construction methods. In Concrete Innovation Conference CIC (pp. 11-13).

Pradhan, K. K., & Chakraverty, S. (2019). Computational structural mechanics: static and dynamic behaviors

Pye, S., Li, F. G., Price, J., & Fais, B. (2017). Achieving net-zero emissions through the reframing of UK national targets in the post-Paris Agreement era. Nature energy, 2(3), 1-7.

Ramage, M. H., Burridge, H., Busse-Wicher, M., Fereday, G., Reynolds, T., Shah, D. U., ... & Scherman, O. (2017). The wood from the trees: The use of timber in construction. Renewable and Sustainable Energy Reviews, 68, 333-359.

Rapp, B. E. (2022). Microfluidics: modeling, mechanics and mathematics. Elsevier.

Schänzlin, J., & Dias, A. M. P. G. (2022, May). Design of Timber-Concrete-Composite Structures. In Proceedings of the 4th International Conference on Timber Bridges, Biel/Bienne, Switzerland (pp. 9-12).

Spasojevic, A. (2008). Structural implications of ultra-high-performance fibre-reinforced concrete in bridge design (No. THESIS). Epfl.

Standard, N. (1998). Norwegian Council for building standardization. NS3473, Norw.

Taylor J (2003) Review of the environmental impact of wood compared with alternative products used in the production of furniture. Forest and Wood Products Research and Development Coorporation, Australia

Tennis, P. D., Leming, M. L., Akers, D. J., Pervious Concrete Pavements," Portland Cement Association, & National Ready Mixed Concrete Association. (2004). Skokie. Illinois, and National Ready Mixed Concrete Association, Maryland, USA, Silver, 36

The Norwegian Standard. (2016). Structural timber—strength classes. Norwegian Standard NS-EN, 338.

Thompson, M. K., & Thompson, J. M. (2017). ANSYS mechanical APDL for finite element analysis. Butterworth-Heinemann.

Timber, H. N. (2022). Glued Laminated Timber. The Engineering Timber Beam, Germany. Available online: https://www. hess-timber. com/en/products/glued-laminated-timber/(accessed on 29 September 2021). (pp.10)

Tsalkatidis, T. (2014). Numerical simulation and analytical study of glulam timber beams. International Journal of Engineering & Technology, 3(2), 129.

Tsalkatidis, T., Amara, Y., Embaye, S., & Nathan, E. (2018). Numerical investigation of bolted hybrid steel-timber connections. Frontiers in built environment, 4, 48.

United Nations Environment Program. (2021). Global status report for buildings and construction. Global Alliance for Building and Construction.

Wang, H. (2004). Theoretical evaluation of embedded plate-like and solid cylindrical concrete structures with guided waves. Northwestern University.

Wickeler, A. L., & Naguib, H. E. (2020). Novel origami-inspired metamaterials: Design, mechanical testing and finite element modelling. Materials & Design, 186, 108242.

Yeoh, D., Fragiacomo, M., De Franceschi, M., & Heng Boon, K. (2011). State of the art on timber-concrete composite structures: Literature review. Journal of structural engineering, 137(10), 1085-1095.

Yuan, Q., Liu, Z., Zheng, K., & Ma, C. (2021). Civil Engineering Materials: From Theory to Practice. Elsevier. Chapter 5. (PP. 240-259)

Zhang, Y., Wang, F., Huang, H., Guo, Y., Li, B., Liu, Y., & Chu, P. K. (2016). Gypsum blocks produced from TiO2 production by-products. Environmental technology, 37(9), 1094-1100.

Zhu, E. C., Guan, Z. W., Rodd, P. D., & Pope, D. J. (2005). A constitutive model for OSB and its application in FE analysis. Wood as raw material and material, 63, 87-93.
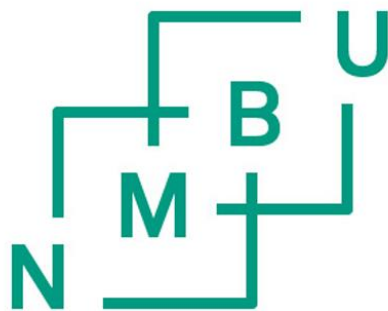
Norges miljø- og
biovitenskapelige
universitet